

New *p*-Methylsulfonamido Phenylethylamine Analogues as Class III Antiarrhythmic Agents: Design, Synthesis, Biological Assay, and 3D-QSAR Analysis

Hong Liu,[†] Ming Ji,[‡] Xiaomin Luo,[†] Jianhua Shen,[†] Xiaoqin Huang,[†] Weiyi Hua,^{*,‡} Hualiang Jiang,^{*,†} and Kaixian Chen[†]

Center for Drug Discovery and Design, The State Key Laboratory of Drug Research, Shanghai Institute of Materia Medica, Shanghai Institutes for Biological Sciences, Chinese Academy of Sciences, Shanghai 200031, People's Republic of China, and Department of Medicinal Chemistry, China Pharmaceutical University, Nanjing 210009, China

Received December 19, 2001

Class III antiarrhythmic agents selectively delay the effective refractory period (ERP) and increase the transmembrane action potential duration (APD). Using dofetilide (**2**) as a template of class III antiarrhythmic agents, we designed and synthesized 16 methylsulfonamido phenylethylamine analogues (**4a–d** and **5a–l**). Pharmacological assay indicated that all of these compounds showed activity for increasing the ERP in isolated animal atrium; among them, the effective concentration of compound **4a** is 1.6×10^{-8} mol/L in increasing ERP by 10 ms, slightly less potent than that of **2**, 1.1×10^{-8} mol/L. Compound **4a** also produced a slightly lower change in ERP at 10^{-5} M, $\Delta\text{ERP}\% = 17.5\%$ ($\Delta\text{ERP}\% = 24.0\%$ for dofetilide). On the basis of this bioassay result, these 16 compounds together with dofetilide were investigated by the three-dimensional quantitative structure–activity relationship (3D-QSAR) techniques of comparative molecular field analysis (CoMFA), comparative molecular similarity index analysis (CoMSIA), and the hologram QSAR (HQSAR). The 3D-QSAR models were tested with another 11 compounds (**4e–h** and **5m–s**) that we synthesized later. Results revealed that the CoMFA, CoMSIA, and HQSAR predicted activities for the 11 newly synthesized compounds that have a good correlation with their experimental value, $r^2 = 0.943$, 0.891 , and 0.809 for the three QSAR models, respectively. This indicates that the 3D-QSAR models proved a good predictive ability and could describe the steric, electrostatic, and hydrophobic requirements for recognition forces of the receptor site. On the basis of these results, we designed and synthesized another eight new analogues of methanesulfonamido phenylethylamine (**6a–h**) according to the clues provided by the 3D-QSAR analyses. Pharmacological assay indicated that the effective concentrations of delaying the ERP by 10 ms of these newly designed compounds correlated well with the 3D-QSAR predicted values. It is remarkable that the percent change of delaying ERP at 10^{-5} M compound **6c** is much higher than that of dofetilide; the effective concentration of compound **6c** is 5.0×10^{-8} mol/L in increasing the ERP by 10 ms, which is slightly lower than that of **2**. The results showed that the 3D-QSAR models are reliable and can be extended to design new antiarrhythmic agents.

Introduction

The high incidence of sudden cardiac death (SCD) is of continuing medical concern.^{1,2} The primary mechanism of SCD is the degeneration of a normal cardiac rhythm into ventricular tachycardia followed by ventricular fibrillation. The cause underlying these rhythm disturbances in most cases is coronary artery disease, which has resulted in prior ischemic damage to the heart.^{3,4} Therefore, it has been accepted that arrhythmias such as sustained tachycardia (VT) and fibrillation (VF) are the major origins in these deaths.⁵ A number of therapeutic approaches are available for the treatment of arrhythmias. According to the classification of Vaughn Williams,⁶ the antiarrhythmic action can be defined by several major classes: class I consists of antiarrhythmic agents that block sodium channels, and

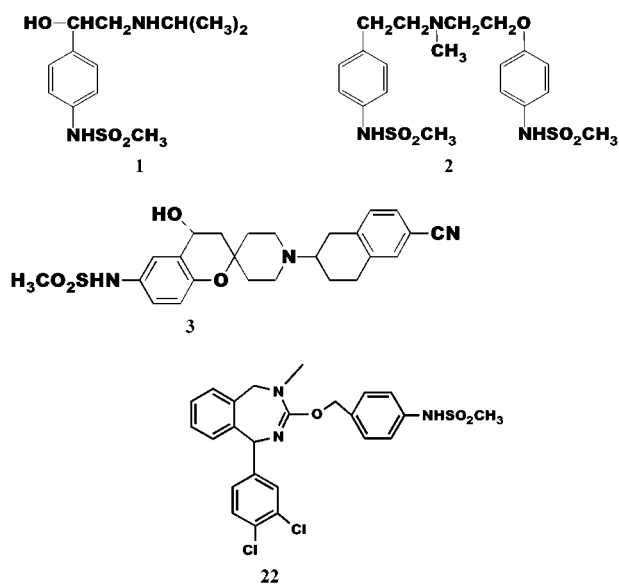
these agents inhibit the impulse conduction and contractility in the myocardium; class II agents are β blockers; and class III agents act through delaying repolarization of cardiac myocytes. The consequence of delayed repolarization is a lengthening of the action potential duration (APD) of the cell and a concomitant increase in the effective refractory period (ERP).⁷ The cardiac arrhythmia suppression trial (CAST) demonstrated that conventional antiarrhythmic treatment with certain class I agents actually increased mortality as compared with placebo.^{8,9} Since the outcome of CAST, a perception has emerged that class I agents may be limited in their therapeutic application; therefore, there has been an increasing interest in compounds that exert their antiarrhythmic effects by means other than the sodium channel blockade.^{10,11} Because of this, development of new antiarrhythmic drugs has focused upon the potassium ion (K^+) channel blockers designed to prolong ventricular refractoriness and prevent the development of lethal tachyarrhythmias.

* To whom correspondence should be addressed. Tel.: +86-21-64311833 ext. 222. Fax: +86-21-64370269. E-mail: hljiang@mail.shnc.ac.cn, jiang@iris3.simm.ac.cn.

[†] Chinese Academy of Sciences.

[‡] China Pharmaceutical University.

Chart 1



The outward delayed rectifier potassium current, I_K , that contributes to repolarization consists of two kinetically distinct and identifiable currents, i.e., a rapidly activating, I_{Kr} , and a slowly activating, I_{Ks} , component.^{12,13} Selective blockading of either I_{Kr} or I_{Ks} would lead to a prolongation of the refractory period; therefore, K^+ channel blockers can be categorized into class III antiarrhythmic agents.^{14–19} Most selective class III antiarrhythmic agents, notably *D*-sotalol (**1**),¹⁹ dofetilide (**2**),^{20–28} and MK-499 (**3**)¹⁶ (Chart 1), pharmacologically function to selectively block I_{Kr} .²³

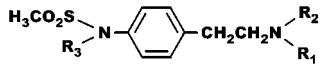
To discover more potent class III antiarrhythmic agents, we have designed and synthesized a series of new methanesulfonamido phenylethylamine analogues based on the structure and pharmacophore of dofetilide. Pharmacological screening indicates that all of these analogues exert significant class III activity in vitro (Table 1). Some of the results have been reported in preliminary form.²⁹ In this paper, we describe in detail the design, synthesis, biological activity, and three-dimensional quantitative structure–activity relationship (3D-QSAR) analyses of dofetilide (**2**) and 35 related novel methanesulfonamido phenylethylamine analogues (**4a–h**, **5a–s**, and **6a–h**). Briefly, we designed and synthesized 17 methanesulfonamido phenylethylamine analogues (**2**, **4a–d**, and **5a–l**) in the first cycle. Pharmacological assay indicated that all of these compounds show the activity in increasing the ERP of isolated animal atrium. Second, on the basis of the bioassay results, these 17 methanesulfonamido phenylethylamine analogues were analyzed by using the 3D-QSAR techniques of comparative molecular field analysis (CoMFA),³⁰ comparative molecular similarity index analysis (CoMSIA),³¹ and the newly developed QSAR method hologram QSAR (HQSAR).³² Then, we synthesized 11 new analogues (**4e–h** and **5m–s**) for testing the 3D-QSAR models. Results indicated that the CoMFA-, CoMSIA-, and HQSAR-predicted activities for the 11 newly synthesized compounds had a good correlation with their experimental value ($r^2 = 0.943$, 0.891 , and 0.809 , respectively). This indicated that the 3D-QSAR models proved a good predictive ability and described the steric, electrostatic, and hydrophobic requirements

for recognition forces of the receptor site. Finally, we designed and synthesized another eight new analogues (**6a–h**) of methanesulfonamido phenylethylamine according to the clues provided by the 3D-QSAR analyses (Table 2). Pharmacological assay indicated that the effective concentrations in delaying the ERP by 10 ms of these newly designed compounds have a good correlation with the 3D-QSAR-predicted values. It is remarkable that compound **6c** is more active than dofetilide in prolonging ERP at 10^{-5} M and its Δ ERP% is 58% (Δ ERP% = 24.0% for dofetilide). The effective concentration of compound **6c** is 5.0×10^{-8} mol/L in increasing the ERP by 10 ms, slightly lower than that of **2**, which is 1.1×10^{-8} mol/L.

Chemistry and Bioassay

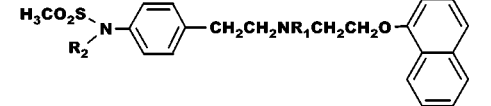
1. Design of Methanesulfonamido Phenylethylamine Analogues. Compound **2** is a class III antiarrhythmic agent, launched into the market by Pfizer as a new antiarrhythmic drug in 1999.^{20–28} The delayed APD and ERP of dofetilide are distinctly superior to other class III antiarrhythmic drugs.^{20–28} The activity of this new drug is about 100–1000 times higher than that of *D*-sotalol (**1**), which can selectively block I_{Kr} without an effect on cardiac conduction and, in addition, lacks a negative inotropic action.^{20–28} Dofetilide is therefore a suitable lead compound for designing new antiarrhythmic agents. Accordingly, on the basis of the structural and pharmacological features of dofetilide, 16 new methanesulfonamido phenylethylamine analogues (**4a–d** and **5a–l**) (Table 1) were designed and synthesized for the first round. Keeping the key groups of dofetilide—the two aromatic rings, alkylamine ether, and two methanesulfonamide groups—we used various steric, electronic, and hydrophobic groups to substitute the *N*-methyl group in dofetilide and obtained four dofetilide analogues **4a–d**. On the basis of the structural features of other class III antiarrhythmic agents, for example, *D*-sotalol (**1**) and MK-499 (**3**), we designed compounds **5a–l**, maintained the methanesulfonamido phenylethylamine moiety, and replaced the methanesulfonamido phenoxyethyl moiety with an alkyl or aromatic alkyl. To test our 3D-QSAR models, we designed an additional 11 new analogues; among them, four are compound **4** analogues (**4e–h**) and seven are compound **5** analogues (**5m–s**). According to the clues suggested by CoMFA, CoMSIA, and HQSAR models, we designed another eight new analogues and represented them as **6a–h** (Table 2).

2. Chemistry. Dofetilide was synthesized using *N*-methyl-*p*-nitrophenethylamine as the starting raw material in Pfizer's patents.²⁰ This synthetic approach is not suitable for structural modification on the *N*-methyl moiety. Therefore, we used *p*-nitrophenethylamine (**8**) as the starting material to synthesize the target compounds **4a–h**. Scheme 1 depicts the sequence of reactions that led to the preparation of the target molecules. In general, 2-(4-nitrophenoxy)-1-bromoethane (**7**) was prepared by *p*-nitrophenol reacting with 1,2-dibromoethane in ethanol. Compound **7** was substituted by using *p*-nitrophenethylamine hydrobromide (**8**), giving the key intermediate **9**. Compounds **10a,b,d–h** were synthesized by the following steps. *N*-Alkylation of **9** with benzyl chloride, acetic anhydride, *p*-chlorobenzyl

Table 1. Chemical Structures of the Methanesulfonamido Phenylethylamine Compounds **2**, **4**, and **5** and Their Activities


compd	R ₁	R ₂	R ₃	n ^a	C ^b	ΔERP ^c	ΔHR ^d	ΔFC ^e
2	-CH ₃	-CH ₂ CH ₂ OC ₆ H ₄ NHSO ₂ CH ₃ - <i>p</i>	H	5	0.011 ± 0.001	24.0 ± 1.0	-30.0 ± 1.6	17.1 ± 0.8
4a	-CH ₂ C ₆ H ₅	-CH ₂ CH ₂ OC ₆ H ₄ NHSO ₂ CH ₃ - <i>p</i>	H	4	0.016 ± 0.001	17.5 ± 0.8	-32.0 ± 1.5	24.8 ± 1.0
4b	-COCH ₃	-CH ₂ CH ₂ OC ₆ H ₄ NHSO ₂ CH ₃ - <i>p</i>	H	3	0.021 ± 0.001	16.9 ± 0.8	-20.6 ± 0.9	17.5 ± 0.8
4c	-H	-CH ₂ CH ₂ OC ₆ H ₄ NHSO ₂ CH ₃ - <i>p</i>	H	3	0.023 ± 0.001	9.39 ± 0.50	-23.8 ± 1.0	33.7 ± 1.7
4d	-CH ₂ C ₆ H ₄ Cl- <i>p</i>	-CH ₂ CH ₂ OC ₆ H ₄ NHSO ₂ CH ₃ - <i>p</i>	H	2	0.037 ± 0.002	9.29 ± 0.50	-40.6 ± 2.0	20.0 ± 1.0
4e	-CH ₂ CH ₂ OC ₆ H ₄ NHSO ₂ CH ₃ - <i>p</i>	-CH ₂ CH ₂ OC ₆ H ₄ NHSO ₂ CH ₃ - <i>p</i>	H	2	0.383 ± 0.020	13.5 ± 0.7	-26.7 ± 2.0	20.0 ± 1.0
4f	-SO ₂ CH ₃	-CH ₂ CH ₂ OC ₆ H ₄ NHSO ₂ CH ₃ - <i>p</i>	H	2	N ^f	N ^f	-18.8 ± 0.8	16.7 ± 0.7
4g	-CH ₂ -CH=CH ₂	-CH ₂ CH ₂ OC ₆ H ₄ NHSO ₂ CH ₃ - <i>p</i>	H	2	0.267 ± 0.010	12.4 ± 0.6	-5.26 ± 0.25	N ^f
4h	-COC ₆ H ₅	-CH ₂ CH ₂ OC ₆ H ₄ NHSO ₂ CH ₃ - <i>p</i>	H	3	0.039 ± 0.002	19.0 ± 0.9	-28.4 ± 1.2	25.0 ± 1.2
5a	-CH ₃	-CH ₂ C ₆ H ₅	H	2	0.372 ± 0.020	12.2 ± 0.6	-20.0 ± 0.9	16.7 ± 0.8
5b	-CH ₃	-CH ₂ C ₆ H ₄ CH ₃ - <i>p</i>	-SO ₂ CH ₃	2	0.953 ± 0.050	12.6 ± 0.7	-15.4 ± 0.8	-11.8 ± 0.7
5c	-CH ₃	-CH ₂ C ₆ H ₄ Cl- <i>p</i>	-H	2	2.24 ± 0.130	7.06 ± 0.30	-14.5 ± 0.7	8.33 ± 0.40
5d	-CH ₃	-CH ₂ C ₆ H ₄ OCH ₃ - <i>p</i>	-SO ₂ CH ₃	2	1.17 ± 0.060	8.70 ± 0.40	-19.2 ± 0.8	25.0 ± 1.2
5e	-CH ₃	-C ₆ H ₁₁	-H	2	4.79 ± 0.300	6.45 ± 0.30	-8.00 ± 0.50	8.33 ± 0.50
5f	-CH ₃	-CH ₂ C ₆ H ₃ OCH ₂ O-3,4	-H	2	0.890 ± 0.050	6.16 ± 0.20	-15.3 ± 0.6	17.2 ± 0.6
5g	-CH ₂ C ₆ H ₅	-CH ₂ C ₆ H ₄ OCH ₃ - <i>o</i>	-H	2	0.141 ± 0.007	10.9 ± 0.6	-28.2 ± 1.0	-14.3 ± 0.6
5h	-CH ₂ C ₆ H ₅	-CH ₂ C ₆ H ₅	-H	2	0.270 ± 0.010	16.1 ± 0.6	-25.0 ± 1.2	N ^f
5i	-CH ₂ C ₆ H ₅	-CH ₂ C ₆ H ₄ CH ₃ - <i>p</i>	-SO ₂ CH ₃	2	0.620 ± 0.030	5.71 ± 0.20	16.0 ± 0.7	25.0 ± 1.2
5j	-CH ₂ C ₆ H ₅	-CH ₂ C ₆ H ₄ Cl- <i>p</i>	-H	2	1.05 ± 0.050	14.5 ± 0.6	16.0 ± 0.8	25.0 ± 1.2
5k	-CH ₂ C ₆ H ₅	-CH ₂ C ₆ H ₄ OCH ₃ - <i>p</i>	-SO ₂ CH ₃	2	0.790 ± 0.050	9.09 ± 0.40	-27.3 ± 1.2	-20.0 ± 1.0
5l	-CH ₂ C ₆ H ₅	-CH ₂ C ₆ H ₃ OCH ₂ O-3,4	-SO ₂ CH ₃	2	0.380 ± 0.030	9.46 ± 0.40	-18.3 ± 0.7	-20.0 ± 1.0
5m	-CH ₂ C ₆ H ₅ Cl- <i>p</i>	-CH ₂ C ₆ H ₄ OCH ₃ - <i>p</i>	-H	2	0.068 ± 0.003	19.3 ± 0.9	-9.09 ± 0.50	15.0 ± 0.6
5n	-CH ₃	-CH ₂ C ₆ H ₄ OCH ₃ - <i>o</i>	-H	3	0.155 ± 0.005	15.6 ± 0.6	-26.7 ± 1.7	38.3 ± 2.0
5o	-COCH ₃	-CH ₂ C ₆ H ₄ OCH ₃ - <i>p</i>	-H	2	N ^f	N ^f	-18.2 ± 0.7	14.3 ± 0.6
5p	-COC ₆ H ₅	-CH ₂ C ₆ H ₄ OCH ₃ - <i>p</i>	-H	2	6.18 ± 0.300	6.33 ± 0.30	-3.70 ± 0.20	33.3 ± 2.0
5q	-CH ₃	-C ₆ H ₁₁	-SO ₂ CH ₃	2	4.39 ± 0.200	6.24 ± 0.30	-8.36 ± 0.50	N ^f
5r	-CH ₂ C ₆ H ₅	-CH ₂ C ₆ H ₅	-SO ₂ CH ₃	2	0.653 ± 0.040	9.56 ± 0.40	-16.0 ± 0.7	N ^f
5s	-CH ₂ C ₆ H ₄ OCH ₃ - <i>p</i>	-CH ₂ CH ₂ OC ₆ H ₄ NHSO ₂ CH ₃ - <i>p</i>	H	2	0.21 ± 0.010	12.1 ± 0.6	-25.8 ± 1.7	14.3 ± 0.6

^a n, the sample number. ^b C, the effective concentration of delaying ERP 10 ms (μM). ^c ΔERP, the percent change of delaying ERP at 10⁻⁵ M (%). ^d ΔHR, the percent change of heart rate at 10⁻⁵ M (%). ^e ΔFC, the percent change of force of constriction at 10⁻⁵ M (%). ^f N, no effect at 10⁻⁵ M.

Table 2. Chemical Structures of Compound **6** and Its Activities


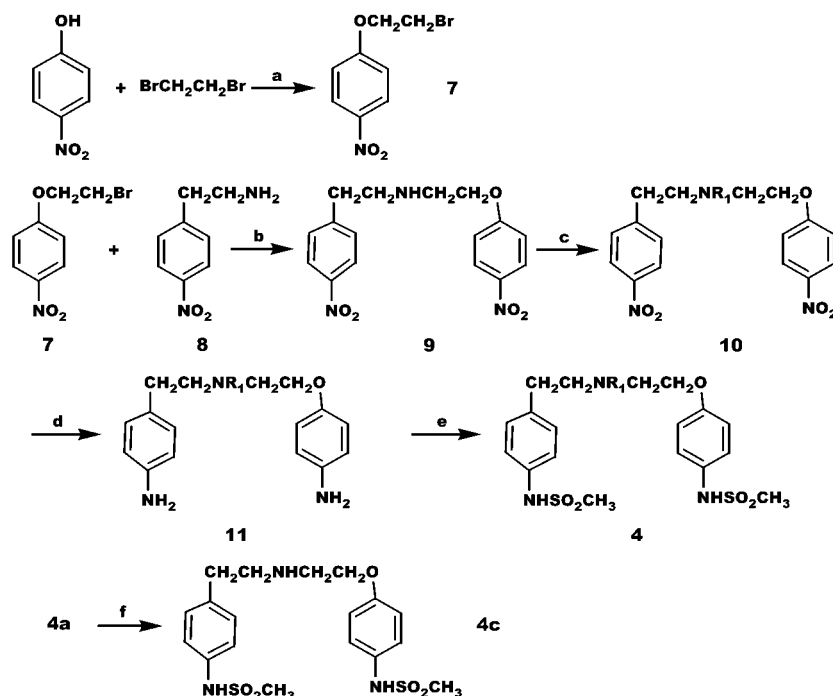
compd	R ₁	R ₂	n ^a	C ^b	ΔERP ^c	ΔHR ^d	ΔFC ^e
6a	-CH ₃	-H	3	0.293 ± 0.010	20.2 ± 1.2	-28.5 ± 1.5	20.3 ± 1.0
6b	-CH ₂ C ₆ H ₅	-H	3	N ^f	N ^f	-31.8 ± 2.0	25.0 ± 1.2
6c	-COCH ₃	-H	3	0.05 ± 0.01	58.4 ± 2.0	-46.2 ± 2.0	-37.9 ± 2.0
6d	-CH ₂ CH=CH ₂	-H	2	0.315 ± 0.010	9.77 ± 0.50	-15.2 ± 0.6	16.7 ± 0.6
6e	-CH ₂ CH=CH ₂	-SO ₂ CH ₃	2	N ^f	N ^f	-8.33 ± 0.40	16.7 ± 0.6
6f	-COC ₆ H ₅	-H	2	8.67 ± 0.40	5.33 ± 0.20	-20.0 ± 1.0	33.3 ± 2.0
6g	-CH ₂ C ₆ H ₅	-SO ₂ CH ₃	2	N ^f	N ^f	-17.9 ± 0.9	25 ± 1
6h	-CH ₃	-SO ₂ CH ₃	2	0.203 ± 0.010	12.0 ± 0.6	-20.7 ± 1.0	N ^f

^a n, the sample number. ^b C, the effective concentration of delaying ERP 10 ms (μM). ^c ΔERP, the percent change of delaying ERP at 10⁻⁵ M (%). ^d ΔHR, the percent change of heart rate at 10⁻⁵ M (%). ^e ΔFC, the percent change of force of constriction at 10⁻⁵ M (%). ^f N, no effect at 10⁻⁵ M.

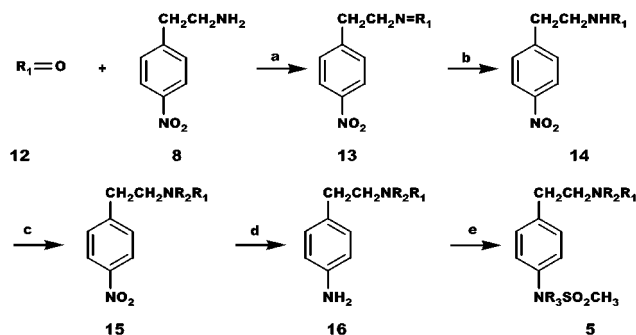
chloride, allyl bromide, and benzoyl chloride was conducted by refluxing with K₂CO₃ in acetone, which afforded compounds **10a,b,d-h**, respectively, which were then reduced by Fe in hydrochloric acid. Finally, the analogues of compound **4** were furnished by methylsulfonation in triethylamine. Compound **4** is thermally unstable and should be handled in an ice bath. Compound **4a** was reduced with Pd-C in hydrogen at one atmosphere pressure, affording compound **4c**. Compound **5** was synthesized through the route outlined in Scheme 2. Phenylaldehydes (**12**) react with *p*-nitrophenylethylamine (**8**), forming Schiff base **13**, which was reduced with KBH₄ to produce compound **14**; then, when steps c-e of Scheme 1 were employed, the target compounds **5a-s** were obtained. Compounds **6a-h** were synthesized through the route outlined in Scheme 3.

They were synthesized by using the same approach as analogues of compound **4**, except *p*-nitrophenol was replaced by α-naphthol (**17**). *N*-Methylation of compound **20a** was performed with satisfactory yields in formate after the N atom of the amine of compound **19** was generated with formaldehyde, giving compound **20a**.

3. Biological Assay. Guinea pigs of either sex (250–350 g) were stunned for quick heart excision. The dissected left atria were attached to small platinum-iridium punctuated electrodes for local depolarization. They were suspended together with the spontaneously beating right atria in an organ bath containing 100 mL of oxygenated Tyrode's solution of the following composition (in mM): NaCl, 147; KCl, 5.4; CaCl₂, 1.8; MgCl₂, 1.05; Tris 10, and Glucose 11. The solution was

Scheme 1^a

^a Reagents and conditions: (a) TBA, EtOH, 46.8%. (b) K_2CO_3 , CH_3CN , reflux, 81.5%. (c) (i) HCHO, HCOOH, reflux, 87.2%; (ii) R_1X , CH_3CN , reflux, 61%; (iii) Ac_2O , CH_3CN , room temperature, 91%. (d) Fe, HCl, EtOH, reflux, 75%. (e) CH_3SO_2Cl , Et_3N , CH_2Cl_2 , 0 °C, 92.3%. (f) CH_3COOH , $H_2/Pd-C$, air pressure, 41.8%.

Scheme 2^a

^a Reagents and conditions: (a) Benzene or EtOH, reflux. (b) KBH_4 , HCl, 86%. (c) (i) HCHO, HCOOH, reflux, 87.2%; (ii) R_1X , CH_3CN , reflux, 61%. (d) Fe, HCl, EtOH, reflux, 75%. (e) CH_3SO_2Cl , Et_3N , CH_2Cl_2 , 0 °C, 92.3%.

continuously bubbled with a mixture of 95% O_2 and 5% CO_2 . The temperature was kept constant at 37 ± 5 °C, and the pH was maintained between 7.2 and 7.4. The atria were connected to a statham strain gauge UC3, preloaded with 10 mN, and isometric contractions were recorded on a polygraph. The left atria were stimulated with a basic frequency of $1 s^{-1}$ by square-wave pulses of 3 min duration and twice-threshold voltage with a type SEN-7103 stimulator (Nihon Kohden corporation). The ERP was measured according to the method of Erich;³³ after every third stimulus, a second test stimulus identical to the first was delivered with increasing delays until it caused an extrasystole that could be identified by postextrasystolic potentiation in response to the following regular stimulus.

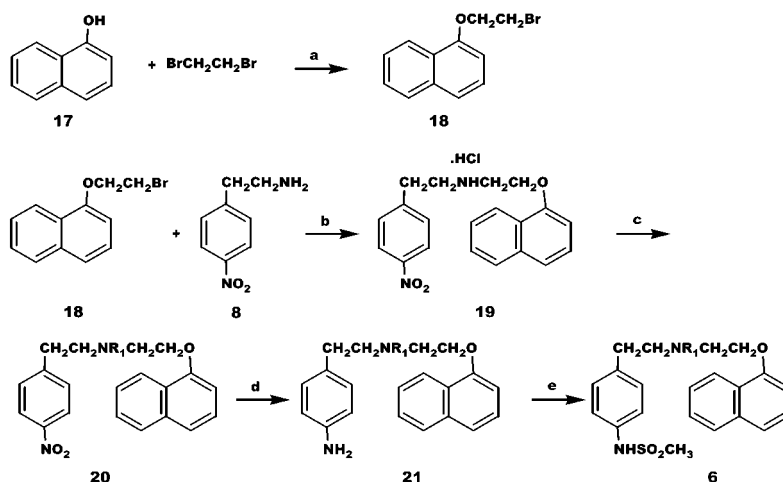
The contraction of the spontaneously beating right atria was recorded at the same time to assess the spontaneous beating rate. Measurements were obtained every 15 min after washout with fresh Tyrode's solution

during a 1 h equilibration period. In 15 min intervals, drug was droplet from a concentrated stock solution to the tissue bath in a cumulative manner so that the final concentration increased geometrically. Inotropic and chronotropic effects as well as the refractory period were determined 10 min after drug addition.

Computational Details

Molecular modeling and QSAR analyses were performed using the program Sybyl 6.7³⁵ on a Silicon Graphics IRIS Indigo XZ R4000 workstation. All energy calculations were performed employing Minimix routine of Sybyl 6.7³⁵ based on the Tripos force field³⁶ and Gasteiger–Hückel charge.³⁶ Geometric optimizations were carried out using Powell first and then conjugate gradient (CG) procedures with a 0.001 kcal/(mol Å) energy gradient convergence criterion and a distance-dependent dielectric constant.

1. Conformational Search and Alignment. Dofetilide and all of our designed and synthesized molecules are very flexible, so it is very difficult to obtain their probable bioactive (binding) conformations for the alignment of 3D-QSAR analyses. Fortunately, Johnson et al.³⁴ have designed and synthesized benzodiazepines derivatives of dofetilide as class III antiarrhythmic agents, which contain much less flexible bonds. Compound **22** is the most potent compound among these benzodiazepines, and its bioactivity is equivalent to that of dofetilide. We assumed that compound **22** and dofetilide share the same binding site because of their structural similarity and similar bioactivity. Accordingly, we selected this compound as the template for the conformational search and for the alignment of the methanesulfonamido phenylethylamine analogues. A systematic search was performed on compound **22** employing the conformational search functionality of Sybyl.³⁵ The

Scheme 3^a

^a Reagents and conditions: (a) TBA, EtOH, 47.4%. (b) K_2CO_3 , CH_3CN , reflux, 81.5%. (c) (i) HCHO, HCOOH, reflux, 87.2%; (ii) R_1X , CH_3CN , reflux, 61%; (iii) Ac_2O , CH_3CN , room temperature, 91%. (d) Fe, HCl, EtOH, reflux, 75%. (e) $\text{CH}_3\text{SO}_2\text{Cl}$, Et_3N , CH_2Cl_2 , 0 °C, 92.3%.

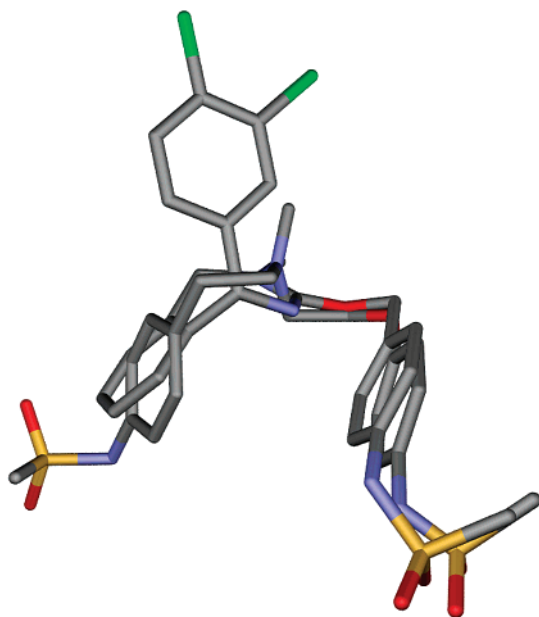


Figure 1. Superposition of the proposed bioactive conformation of dofetilide with the lowest energy conformation of compound 22. This picture was rendered in the POV-Ray program.⁴²

global minimum energy conformation of this molecule was subsequently reoptimized using the Tripos force field³⁶ including the electrostatic term calculated from Gasteiger–Hückel charges.³⁶ Superposed dofetilide (2) with 22 (Figure 1), the dihedral angles in the methylsulfonamido phenoxyethyl moiety (right part) of dofetilide (divided by N atom of 9), τ_4 – τ_6 (Figure 2), can be restricted at 53.4, 55, and 35.2°, respectively. The conformation of the methylsulfonamido phenylethylamine moiety (left part) can be obtained in the following way: taking the distance between C1 and N9 as a restriction, a systematic search was performed about bonds C6–C7, C7–C8, and C8–N9; the lowest energy conformation of dofetilide under the distance constrain, after further geometry optimization with the same method mentioned above, was taken as the possible bioactive conformation. Thus, the geometric parameters of the 3D pharmacophore of dofetilide were obtained

(Figure 2a): $d_1 = 2.958 \text{ \AA}$, $d_2 = 3.793 \text{ \AA}$, and $d_3 = 4.344 \text{ \AA}$, which were considered in the conformational search for other methanesulfonamido phenylethylamine analogues. In this way, the lowest energy conformation for each methanesulfonamido phenylethylamine analogue under the restriction of the dofetilide pharmacophore was isolated as its probable bioactive conformation. After structural optimization, conformational alignment was carried out by taking the pharmacophore of dofetilide mentioned above as the atomic pairs, which were submitted to the following CoMFA,³⁰ CoMSIA,³¹ and HQSAR³² analyses.

2. CoMFA. For the CoMFA calculation, steric and electronic field energies were calculated using an sp^3 carbon as the steric probe atom and a +1 charge for the electrostatic probe. Steric and electrostatic interactions were calculated using the Tripos force field with a distance-dependent dielectric constant at all intersections of a regularly spaced (0.2 nm) grid. The cutoff was set to 30 kcal/mol. All models were investigated using a full cross-validated partial least-squares (PLS)^{37,38} method (leave-one-out) with CoMFA standard options for scaling of variables. Minimum σ (column filtering) was set to 2.0 kcal/mol to improve the signal-to-noise ratio by omitting those lattice points whose energy variation was below this threshold. The optimal number of components was five. The final model (non-cross-validated conventional analysis) was developed and yielded the highest non-cross-validated r^2 value with the optimum number of components equal to that yielding the highest r_{cv}^2 .

3. CoMSIA. The alignment of the CoMFA also served to compute similarity index fields for CoMSIA analysis. In this study, three physicochemical properties, steric, electrostatic, and hydrophobic fields, have been evaluated. The steric contribution was reflected by the third power of the atomic radii of the atoms. Electrostatic properties were introduced as atomic charges. An atom-based hydrophobicity was assigned according to the parametrization developed by Viswanadhan et al.³⁹ The lattice dimensions were selected with a sufficiently large margin (>4 Å) to enclose all aligned molecules. For CoMSIA fields, any singularities were avoided at atomic

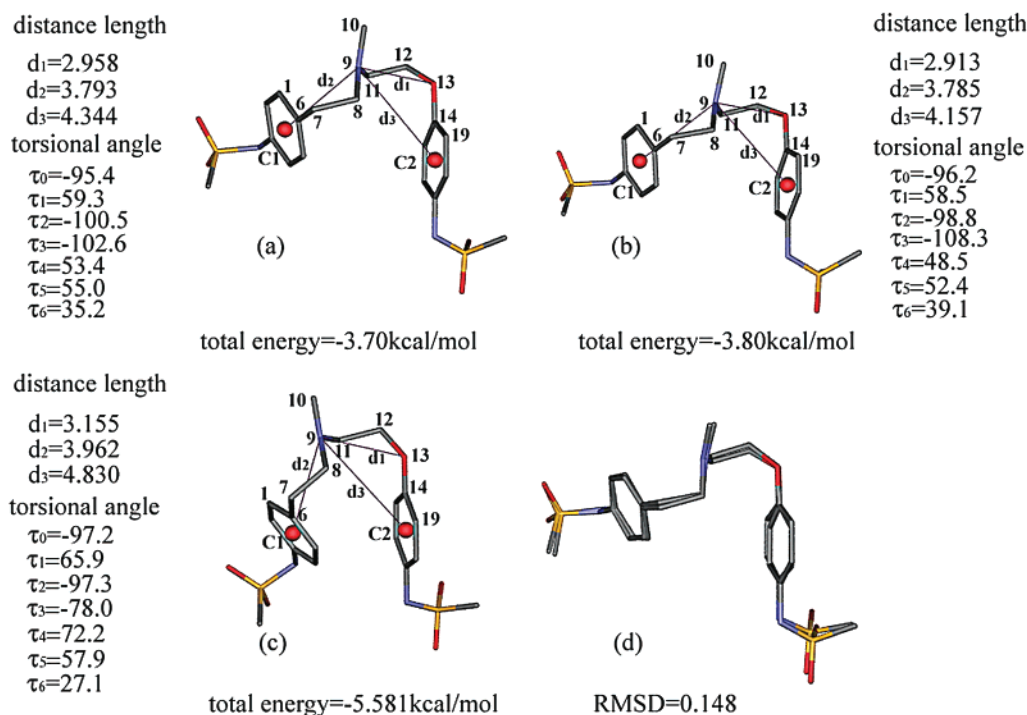


Figure 2. Energetic and geometric parameters of the probable binding (bioactive) conformations (a), corresponding local energy minimum conformations (b), and global energy minimum conformations (c) of dofetilide. Panel d is the probable bioactive conformation of dofetilide superposing with a local energy minimum conformation derived from systematic search. τ_0 : C₁-C₆-C₇-C₈; τ_1 : C₆-C₇-C₈-N₉; τ_2 : C₇-C₈-N₉-C₁₁; τ_3 : C₈-N₉-C₁₁-C₁₂; τ_4 : N₉-C₁₁-C₁₂-O₁₃; τ_5 : C₁₁-C₁₂-O₁₃-C₁₄; and τ_6 : C₁₂-C₁₃-C₁₄-C₁₉. This picture was rendered in POV-Ray software.⁴²

positions because a Gaussian type distance dependence of the physicochemical properties was adopted; thus, no arbitrary cutoffs were required. In general, similarity indices $A_{F,k}$ between the compounds of interest and a probe atom placed at the intersections of the lattice could be calculated with eq 1

$$A_{F,k}^q(j) = -\sum_{i=1}^n w_{\text{probe},k} w_{ik} e^{-ar_{ij}^2} \quad (1)$$

where q represents a grid point; i is the summation index over all atoms of the molecule j under computation; w_{ik} is the actual value of the physicochemical property k of atom i ; and $w_{\text{probe},k}$ is the value of the probe atom. In the present study, similarity indices were computed using a probe atom ($w_{\text{probe},k}$) with charge +1, radius 1 Å, hydrophobicity +1, and attenuation factor α 0.3 for the Gaussian type distance. The statistical evaluation for the CoMSIA analyses was performed in the same way as described in CoMFA.

4. HQSAR. The construction of a molecular hologram containing the HQSAR descriptors was carried out by the following procedure. First, the molecule was hashed to a molecular fingerprint that encoded the frequency of occurrence of various molecular fragment types using a predefined set of rules. This molecular fingerprint was cut into strings at a fixed interval as specified by a hologram length (HL) parameter. All generated strings were then hashed into a fixed length array to produce the molecular hologram. The Sybyl line notation (SLN) for each string generated was mapped to a unique integer in the range of 0 to 2³⁹ using a cyclic redundancy check (CRC) algorithm. The numerical representation of molecules was exploited by a subsequent correlation

analysis; typically, a PLS QSAR model was constructed. The optimal HQSAR model was derived from screening through the 12 default HL values, which were a set of prime numbers ranging from 53 to 401.

Results and Discussion

1. Chemistry and Biology. The chemical formulas of the initially synthesized 17 compounds, denoted with **2**, **4a–d**, and **5a–l**, are listed in Table 1. They were synthesized through the routes outlined in Schemes 1 and 2, and the detailed synthetic procedures and the structural characterizations were described in the following Experimental Section. The effective concentrations of these 17 methanesulfonamido phenylethylamine analogues upon increasing ERP of isolated animal atrium were evaluated utilizing a pair-electric stimulus technique (Table 1). The results show that all of the compounds exhibit antiarrhythmic activity. The effective concentration of compound **4a** is 1.6×10^{-8} mol/L in increasing ERP by 10 ms, slightly less potent than that of **2**, which is 1.1×10^{-8} mol/L, and it produces a slightly lower change in ERP at 10^{-5} M, $\Delta\text{ERP}\% = 17.5\%$ ($\Delta\text{ERP}\% = 24.0\%$ for dofetilide) (Figure 3a). Later, we synthesized another 11 compounds (**4e–h** and **5m–s**) through the routes outlined in Schemes 1 and 2, and the detailed synthetic procedures and the structural characterizations were also described in the Experimental Section. Among these 11 compounds (**4e–h** and **5m–s**), compounds **4h** and **5m** are the most interesting. They are 4–6-fold less potent than dofetilide in the concentration needed to prolong ERP by 10 ms, but they are only slightly less potent than dofetilide in the prolongation of ERP at 10^{-5} M; the $\Delta\text{ERP}\%$ values for these two compounds are, respectively, 19.0 and 19.3% (Table 1). Moreover, compounds **4a,h** and **5m**

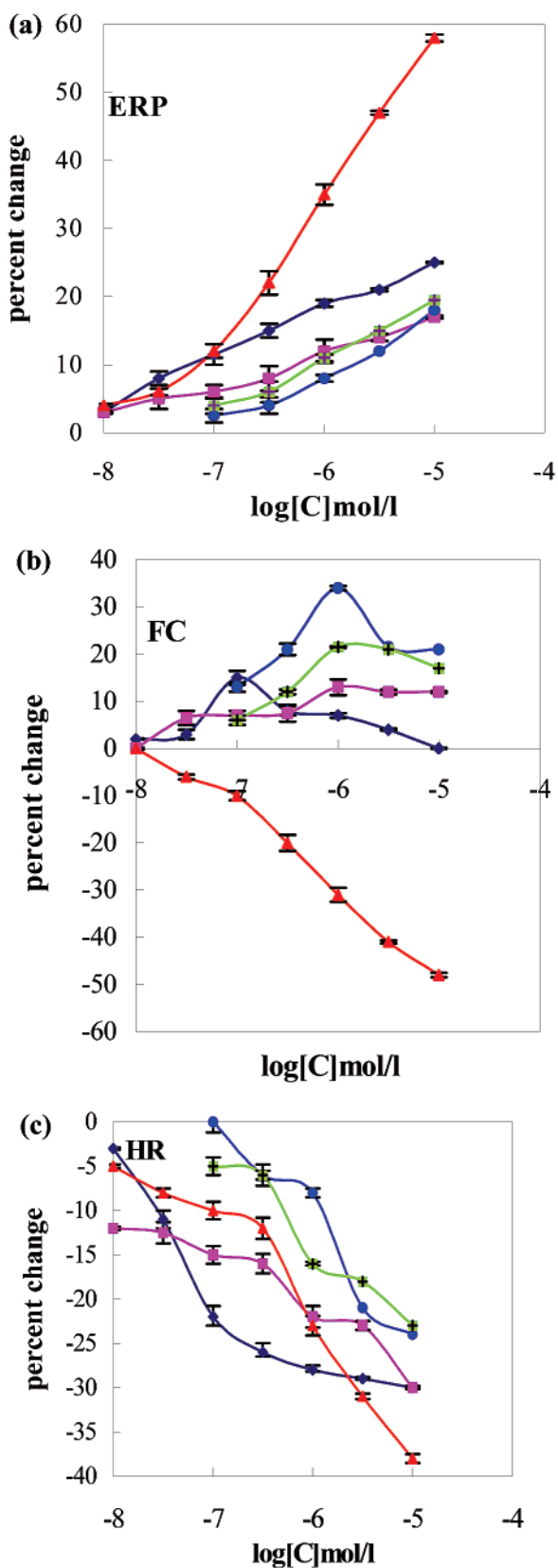


Figure 3. Curves of quantity–effect of compounds **2**, **4a**, **4h**, **5m**, and **6c** bioactivities measured in isolated animal atrium (dark blue diamond, compound **2**; pink square, compound **4a**; blue circle, compound **4h**; green square, compound **5m**; red triangle, compound **6c**). (a) The ERP curves of quantity–effect of five compounds. (b) The FC curves of quantity–effect of five compounds. (c) The HR curves of quantity–effect of five compounds.

prolong ERP, reduce the heart rate, and strengthen cardiac muscle constriction (Table 1 and Figure 3). The curves of quantity–effect are similar to dofetilide (Figure 3).

2. 3D Pharmacophore of Dofetilide Analogues.

The two methylsulfonamido groups are very important pharmacophoric elements for the dofetilide analogues.^{20–28} Because these two methylsulfonamido groups are separated respectively by two aromatic rings from the middle part of dofetilide (alkylamine ether moiety), the conformations of these two parts actually do not influence each other and also do not influence the conformation of the alkylamine ether moiety, especially once the compound binds to the receptor. Therefore, the systematic search for the two methylsulfonamido group “ends” of the dofetilide was carried out separately to save computational time, and the lowest energy conformations of these two ends were adopted in the probable bioactive conformation for the dofetilide analogues. In the following, we just pay attention to the conformation of the alkylamine ether moiety of the compounds in this study.

Besides the double methylsulfonamido groups, one or two hydrophobic aromatic groups (the centroids are denoted as C1 and C2, respectively), a nitrogen atom and an oxygen atom (labeled as N9 and O13 in Figure 2), are the basic pharmacophoric elements. Therefore, the distances between N9 and O13 (d_1), N9 and C1 (d_2), and N9 and C2 (d_3) play an important role for the dofetilide analogues interacting with their receptor. Under the restrictions of d_2 and torsion angles τ_4 – τ_6 derived from the lowest energy conformation of **22**, a probable bioactive conformation of dofetilide was obtained by using the systematic search, which is presented in Figure 2a. The pharmacophoric distances d_1 – d_3 are 2.958, 3.793, and 4.344 Å, respectively.

Typically, the conformation representing the pharmacophore is not always the global energy minimum; however, it may be at or near a local energy minimum conformation. We therefore performed a systematic conformational search for dofetilide considering the flexibility of the torsion angles of all of the single bonds. Different from the proposed bioactive conformation, the global energy minimum conformation of dofetilide adopts a more “crooked” conformation, and its total energy is -5.6 kcal/mol (Figure 2c). As compared with all of the conformations obtained in the systematic search, we found that the proposed bioactive conformation is close to a local energy minimum conformation. The energy of this local energy minimum is about -3.8 kcal/mol, which is very close to that of the proposed bioactive conformation, -3.7 kcal/mol (Figure 2b). The superposition between these two conformations is shown in Figure 2d, and the RMSD is only 0.148 Å. All of these indicate the reasonability of the proposed bioactive conformation of dofetilide.

Obtaining the probable bioactive conformation and the 3D pharmacophore (d_1 – d_3), a systematic search was performed for each of the other 16 methylsulfonamido phenylethylamine analogues taking the 3D pharmacophore as the geometric restriction. The lowest energy conformations under the geometric restriction were adopted in the conformation alignment for 3D-QSAR analyses; during this process, the 3D pharmacophore

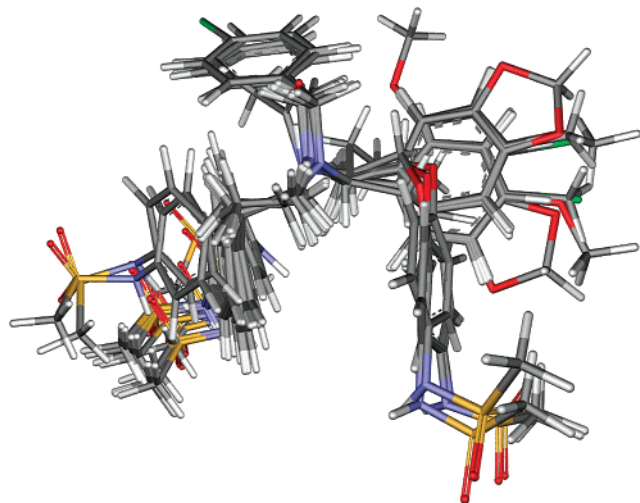


Figure 4. Superposition of the 17 methanesulfonamido phenylethylamine compounds (**2**, **4a–d**, and **4a–l** in Table 1) for 3D-QSAR model construction. This picture was reproduced by the POV-Ray program.⁴²

was taken as the alignment pairs. The conformational alignment is shown in Figure 4.

3. 3D-QSAR Models. 3.1. CoMFA. Although CoMFA is not able to appropriately describe all of the binding force, because it is based principally on standard steric and electrostatic molecular fields to model ligand–enzyme interactions, it is still a widely used tool for the study of QSAR at the 3D level. The major objective of CoMFA analysis about methylsulfonamido phenylethylamine analogues is to find the best predictive model of these analogues. For our initially synthesized 17 compounds (**2**, **4a–d**, and **5a–l**), PLS^{37,38} was used in conjunction with leave-one-out to obtain the optimal number of components for the subsequent analysis. PLS^{37,38} analysis based on least-squares fit gave a correlation with a cross-validated r^2 of 0.695 with the maximum number of components of five. The non-cross-validated PLS analysis was repeated with the optimum number of components, as determined by the cross-validated analysis, to give an r^2 value of 0.985, $F = 144$, and the estimated standard error is 0.125. These values indicated a good conventional statistical correlation, and the CoMFA model has a fair predictive ability. The steric field descriptors (1320 variables) explain 55.1% of the variance, while the electrostatic descriptors explain 44.9% showing a balance between both effects. These statistical parameters and the non-cross-validated predictions are listed in Tables 3 and 4 and shown in Figures 5 and 6.

The CoMFA steric and electrostatic fields for the analysis based on alignments of the proposed bioactive conformations are presented as contour plots in Figure 5. To aid in visualization, the lead compound dofetilide (**2**) is displayed in maps. In general, the colored polyhedra in the map surrounded all lattice points where the QSAR strongly associated changes in the compounds' field values with changes in biological potency. Green polyhedra surrounded regions where more bulk is "good" for increasing potency, while yellow polyhedra surrounded regions where less bulk is "good". In Figure 5, a big region of green contour near the phenyl moiety of phenoxyethane suggests that more potent analogues may be obtained by introducing bulky substitutes to this

Table 3. Statistical Indexes of CoMFA, CoMSIA, and HQSAR Models of 17 Methanesulfonamido Phenylethylamine Compounds

	cross-validated		conventional		
	r_{cross}^2	opt compt	r^2	s	$F_{6,18}$
CoMFA	0.695	5	0.985	0.125	144
CoMSIA	0.700	4	0.970	0.169	96.8
HQSAR	0.810	4	0.921	0.255	353 (BL) ^a
Field Contributions (%)					
	electrostatic	steric	hydrophobic		
CoMFA	44.9	55.1	-		
CoMSIA	46.5	27.1	26.4		

^a The best length in the HQSAR model.

Table 4. Predicted Activities (PA) vs Experimental Activities (EA, $-\log\text{IC}_{50}$) and Residues (δ) by CoMFA, CoMSIA, and HQSAR

compd	CoMFA			CoMSIA		HQSAR	
	EA	PA	δ	PA	δ	PA	δ
2	7.92	7.87	0.05	7.83	0.09	7.75	0.17
4a	7.80	7.89	-0.09	8.02	-0.22	7.86	-0.06
4b	7.67	7.65	0.02	7.68	-0.01	7.65	0.02
4c	7.63	7.60	0.03	7.63	0.00	7.57	0.06
4d	7.44	7.47	-0.03	7.52	-0.08	7.87	-0.43
4e*	6.41	5.92	0.49	6.57	-0.16	6.79	-0.38
4f*	N ^a						
4g*	6.57	6.84	-0.27	6.28	0.29	6.13	0.44
4h*	7.96	7.85	0.11	7.52	0.44	7.63	0.33
5a	6.34	6.31	0.03	6.12	0.22	6.11	0.23
5b	6.02	6.16	-0.14	6.09	-0.07	5.82	0.20
5c	5.65	5.76	-0.11	5.77	-0.12	5.92	-0.27
5d	5.93	5.79	0.14	6.03	-0.10	5.98	-0.05
5e	5.32	5.33	-0.01	5.25	0.07	5.51	-0.19
5f	6.15	6.16	-0.01	6.14	0.01	6.29	-0.14
5g	6.85	6.88	-0.03	6.41	0.44	6.61	0.24
5h	6.57	6.41	0.16	6.32	0.25	6.61	-0.04
5i	6.21	6.12	0.09	6.18	0.03	6.25	-0.04
5j	5.98	6.10	-0.12	6.16	-0.18	5.98	-0.00
5k	6.10	6.08	0.02	6.18	-0.08	6.17	-0.07
5l	6.41	6.42	-0.01	6.29	0.12	6.45	-0.04
5m*	7.17	6.98	0.19	7.45	-0.28	7.36	-0.19
5n*	6.81	6.60	0.21	6.39	0.42	6.61	0.20
5o*	N ^a						
5p*	5.21	5.05	0.16	5.45	-0.24	5.61	-0.40
5q*	5.36	5.24	0.12	5.57	-0.21	5.48	-0.12
5r*	6.19	6.23	-0.04	6.23	-0.04	5.68	0.51
5s*	6.68	6.72	-0.05	6.42	0.26	7.09	-0.41
6a**	6.79	6.67	0.12	7.05	-0.26	6.99	-0.20
6b**	N ^a						
6c**	7.33	7.31	0.02	7.45	-0.12	7.48	-0.15
6d**	6.50	6.53	-0.03	6.46	0.04	6.43	0.07
6e**	N ^a						
6f**	5.06	5.28	-0.21	5.47	-0.41	5.59	-0.53
6g**	6.69	6.50	0.19	6.54	0.15	7.19	-0.50
6h**	6.64	6.66	0.19	6.45	0.19	7.23	-0.59

* Compounds that were not included in the construction of the QSAR models. ** Newly designed compounds according to the CoMFA and CoMSIA models. ^a N, no effect at 10^{-5} M.

region of dofetilide. Red and blue contours show regions of desirable negative and positive electrostatic interactions, respectively. Two red polyhedra near the sulfonyl of methanesulfonamido phenoxyethylamine and O atom of the phenoxyethyl moiety indicate that electron rich groups are beneficial to the activity. Two blue contours near the methyl group of methanesulfonamido phenylethylamine suggest that positively charged substituents are favorable to increase the activity.

3.2. CoMSIA. Similar results were obtained using CoMSIA. To estimate the hydrophobic contributions to

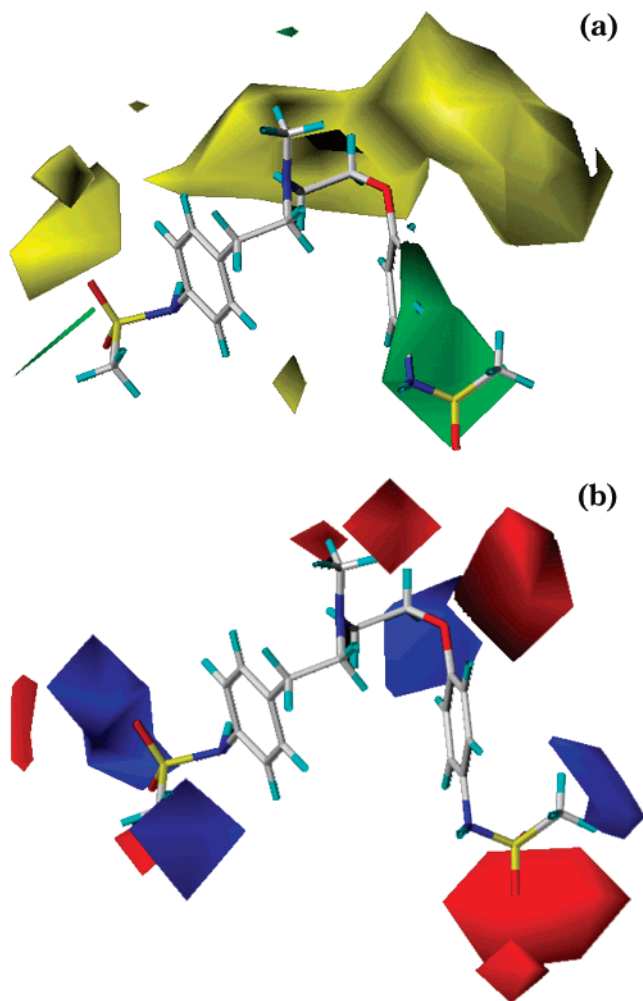


Figure 5. Contour maps from the final CoMFA analysis with 2 Å grid spacing in combination with dofetilide. (a) Steric std*coeff contour map. Green contours (>80% contribution) refer to sterically favored regions; yellow contours (>20% contribution) indicate disfavored areas. (b) Electrostatic std*coeff contour map. Blue contours (>80% contribution) refer to regions where negatively charged substituents are disfavored; red contours (>20% contribution) indicate regions where negatively charged substituents are favored.

these antiarrhythmic compounds, hydrophobic similarity index fields were constructed by use of CoMSIA, which cannot be completely treated by Lennard–Jones and Coulombic fields encoded in CoMFA. The CoMSIA analysis was performed employing the standard options of Sybyl.^{39–41} The results of CoMSIA are shown in Table 3 and Figure 7. Using steric, electrostatic, and hydrophobic descriptors, a CoMSIA model with an r^2 value of 0.700 for four components and a conventional r^2 of 0.970 was obtained. The CoMSIA-derived QSAR of the methanesulfonamido phenylethylamine analogues exhibited a good cross-validated correlation, indicating that it is also highly predictive; the predicted inhibitory activities of these compounds are also listed in Table 4 and graphically shown in Figure 6. The steric field descriptors (1320 variables) explain 27.1% of the variance while the proportion of hydrophobic descriptor remains in the range of 26.4%. Now the additional electrostatic field explains the remaining 46.5% of the variance. Thus, the CoMFA steric field can be seen as a comprehensive contribution of the pure steric and hydrophobic effects because the steric contribution of

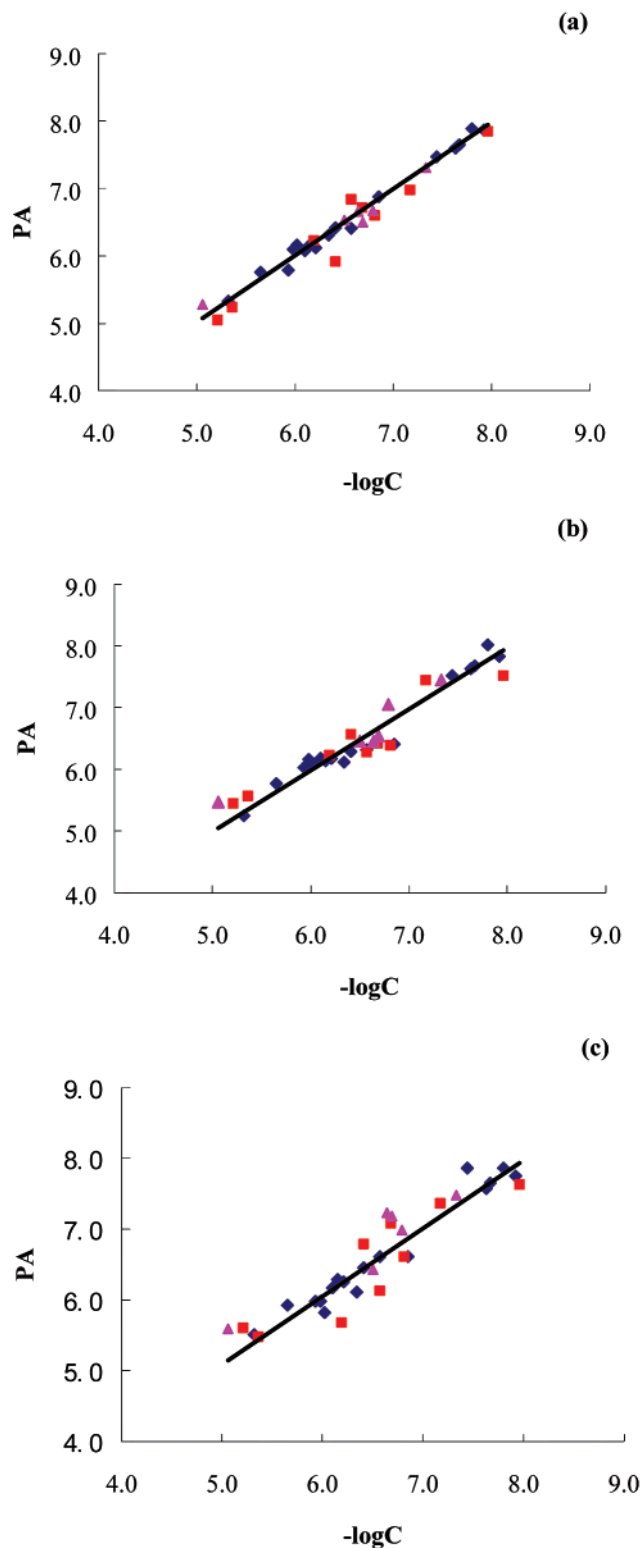


Figure 6. Correlation between predicted activities (PA) by CoMFA (a), CoMSIA (b), and HQSAR (c) models and the experimental activities ($-\log C_{50}$). \blacklozenge , compounds of the training set ($r^2 = 0.989, 0.959,$ and 0.953 for the three QSAR models, respectively); \blacksquare , compounds of the testing set ($r^2 = 0.943, 0.891,$ and 0.809 for the three QSAR models, respectively); \blacktriangle , newly designed compound **6** according to CoMFA and CoMSIA clues ($r^2 = 0.980, 0.909,$ and 0.882 for the three QSAR models, respectively).

CoMFA is 55.1%, which is approximately equal to the summation of the steric and hydrophobic contributions of CoMSIA (53.5%).

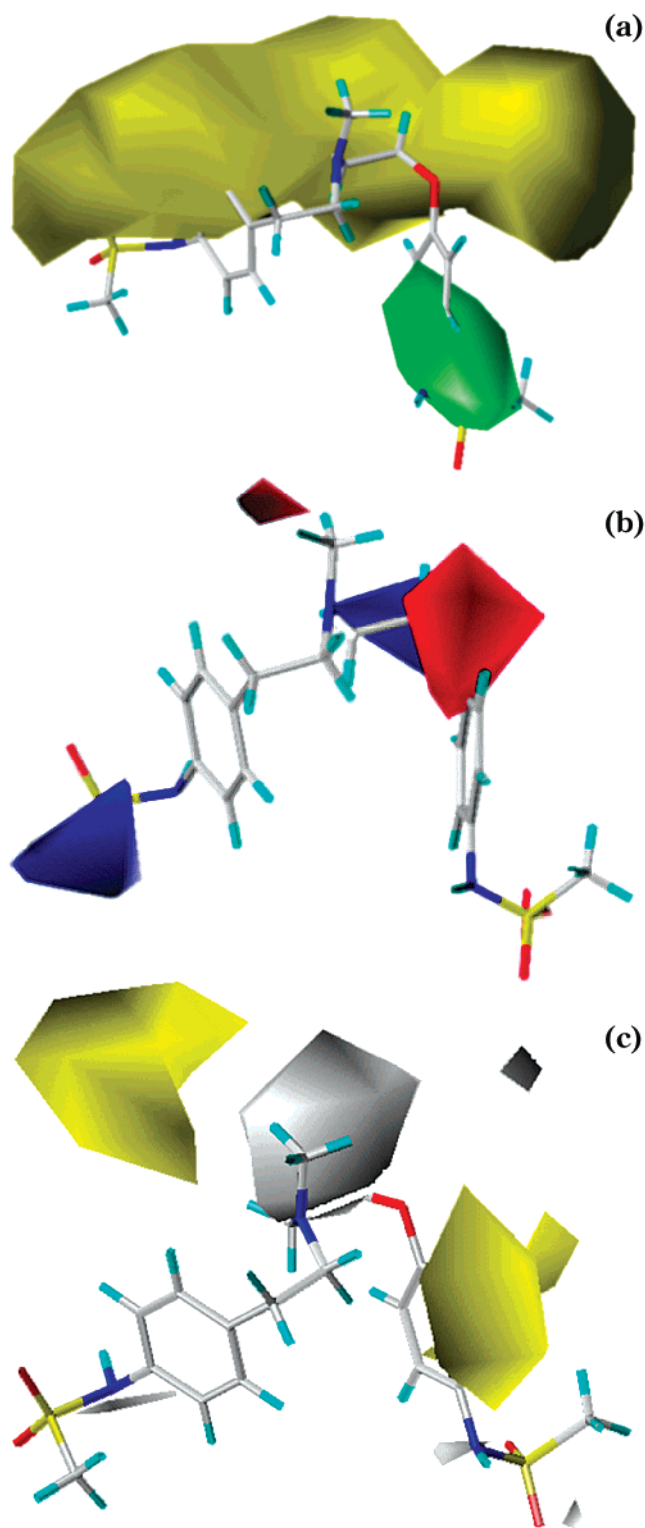


Figure 7. Contour maps from the final CoMSIA analysis with 2 Å grid spacing in combination with dofetilide. (a) Steric std*coeff contour map. Green contours (>80% contribution) refer to sterically favored regions; yellow contours (>20% contribution) indicate disfavored areas. (b) Electrostatic std*coeff contour map. Blue contours (>80% contribution) refer to regions where negatively charged substituents are disfavored; red contours (>20% contribution) indicate regions where negatively charged substituents are favored. (c) Hydrophobic std*coeff contour map. White contours (>80% contribution) refer to regions where hydrophilic substituents are favored; yellow contours (>20% contribution) indicate regions where hydrophobic substituents are favored.

The inspection of CoMSIA steric Std* coeff contour maps shows a high correspondence to the CoMFA results except for the small green contour near the methyl of the *N*-methyl moiety (see Figures 5a and 7a). In general, CoMSIA contours are scattered at the edge of the ligand surface, thus highlighting complementary features at the receptor site. CoMSIA fields can also be represented by color contour plots. In general, yellow polyhedra indicate that hydrophobic substituents are "good" for increasing the potency, while hydrophilic substituents are beneficial to the activity at the regions of white contours. In Figure 7c, large yellow polyhedra around the phenyl of phenoxyethane indicate that enhanced hydrophobic substituents in this region are favorable. A white contour near the methyl of the *N*-methyl moiety suggests that hydrophilic substituents in this position may increase the antiarrhythmic activity.

3.3. HQSAR. The major objective of our HQSAR study is the accurate prediction of the inhibitory activities of the 17 methanesulfonamido phenylethylamine compounds; Table 4 also shows a summary of the results of the HQSAR calculation. These data show that the least standard error occurs at a cross-validated r^2 (q^2) of 0.810 with four optimal components, and the hologram that gives the lowest standard error has a length of 353. The PLS analysis yields a conventional r^2 of 0.921 for the studied compounds. The predicted inhibitory activities of these compounds are also listed in Table 5, and their correlation is shown graphically in Figure 6c. It is important to have a QSAR technique that offers not only a consistent and reproducible prediction but also a fast and convenient procedure. The HQSAR model in our study appears well-suited for such application.

4. Validation of the QSAR Models. To test the stability and predictive ability of the QSAR models derived from the 17 methanesulfonamido phenylethylamine compounds so that they can be employed in new analogue designs, 11 new analogues (**4e–h** and **5m–s**) were synthesized (Schemes 1 and 2, Table 1) as a set of testing for validation. The predicted results are simultaneously shown in Table 4 and Figure 6 (in square pattern-labeled symbols). The predicted values are consistent with the experimental data in a statistically tolerable error range, $r^2 = 0.943, 0.891,$ and 0.809 for CoMFA, CoMSIA, and HQSAR models, respectively. The testing results for these 11 analogues indicate that all of the three QSAR models, CoMFA, CoMSIA, and HQSAR, are reliable and can be used in predicting newly designed compounds.

5. New Analogue Design, Synthesis, and Bioassay. Satisfied by the stability and predictive ability of the QSAR models, we intended to design new analogues based on the clues of CoMFA and CoMSIA. According to CoMFA and CoMSIA analyses (Figures 5 and 7), we can see that adding bulky and hydrophobic groups to the phenyl moiety of phenoxyethane of dofetilide may increase the bioactivity. Following these indications, we designed eight new analogues, denoted as **6a–h** (Table 2). They were synthesized through the route outlined in Scheme 3, and the detailed synthetic procedures and the structural characterizations were described in the Experimental Section. With completion of the synthesis,

in vitro K⁺ channel inhibitory activity of these eight target compounds as compared with dofetilide was measured. According to the method of Wettwer et al.,²⁷ the effective concentration of these eight methanesulfonamido phenylethylamine analogues upon increasing ERP in isolated animal atrium was evaluated utilizing a pair-electric stimulus technique. The results are summarized in Table 2; the bioassay result of compound **6c** is shown in Figure 3. It is remarkable that the percent change of delaying ERP at 10⁻⁵ M of compound **6c** is 58%, which is higher than that of dofetilide, of which the Δ ERP% is 24.02%. The effective concentration of compound **6c** is 5 × 10⁻⁸ mol/L in increasing ERP by 10 ms, slightly lower than that of dofetilide, which is 1.1 × 10⁻⁸ mol/L. Figure 3 shows that compound **6c** prolongs ERP and reduces heart rate and cardiac muscle constriction. The level of prolonging ERP of compound **6c** is much higher than that of dofetilide at 10⁻⁵ M. Reduction in the cardiac muscle constriction of compound **6c** indicates that this compound may block complex K⁺/Ca²⁺ channels.⁴⁴

Conclusion

In summary, we designed and synthesized 16 methylsulfonamido phenylethylamine analogues (**4a–d** and **5a–l**) using **2** as the leading compound. The pharmacological assay indicated that all of these compounds show the activity for increasing the ERP in isolated animal atrium. 3D-QSAR analyses were then performed on dofetilide and the 16 methylsulfonamido phenylethylamine analogues by means of CoMFA, CoMSIA, and HQSAR methods. The 3D-QSAR models proved good predictive abilities in predicting the activity of new compounds. The QSAR models were tested by 11 newly synthesized compounds (**4e–h** and **5m–s**). Results revealed that the CoMFA, CoMSIA, and HQSAR predicted activities for these 11 new analogues had a good correlation with their experimental value, $r^2 = 0.943, 0.891,$ and 0.809 for these three QSAR models, respectively. This indicated that the 3D-QSAR models proved good predictive ability and could describe the steric, electrostatic, and hydrophobic requirements for recognition forces of the receptor site. According to the clues provided by 3D-QSAR analyses, we designed and synthesized a series of new analogues of methanesulfonamido phenylethylamine (**6a–h**). The pharmacological assay indicated that the effective concentration of delaying ERP by 10 ms of these new compounds had a good correlation with the 3D-QSAR predicted data. It was remarkable that the percent change of delaying ERP at 10⁻⁵ M of compound **6c** was much higher than that of dofetilide.

The pharmacological assay for our synthesized compounds was not comprehensive, for we did not determine the APD and ERP on ventricular tissue. However, in this paper, we have shown a comprehensive cycle of active compound design, i.e., construct predictive 3D-QSAR models based on synthesized compounds and their bioactivities; have verified the QSAR models with newly synthesized compounds; have designed and synthesized new active compounds according to the prediction of the QSAR models; and finally have tested the new compounds' activities by using a pharmacological method. The consistency between the predicted data and

the experimental data of our design compounds, especially compound **6c**, showed its better prolongation of ERP than dofetilide, indicating that these compounds are worth further study.

Experimental Section

Reactions were run in flame-dried round-bottomed flasks under a N₂ atmosphere. The reagents (chemicals) were purchased from Shanghai Chemical Reagent Company and used without further purification. Analytical thin-layer chromatography (TLC) was conducted with silica gel 60 F254 plates (250 μ m thickness, Qindao Ocean Chemical Company, China). Yields were not optimized. Melting points were measured in capillary tube and were uncorrected. Infrared (IR) spectra were given using a Perkin-Elmer 983 IR spectrometer and Bruker IFS-48 FT-IR IR spectrometer, and the resonance of both instruments was reported in wavenumbers (cm⁻¹), windows material using potassium bromide (KBr) powder. Nuclear magnetic resonance (NMR) spectra were given on a JEOL F*90 Q FT-NMR and/or ACF* 300Q Bruker NMR (IS as TMS). Chemical shifts were reported in parts per million (ppm, δ) downfield from tetramethylsilane. Splitting patterns were described as singlet (s), doublet (d), triplet (t), quartet (q), multiplet (m), and broad (br). Low- and high-resolution mass spectra (LRMS and HRMS) were given with electric or chemical ionization (EI or CI) produced by Nicolet 2000 model FT-MS spectrometer.

General Procedures for Preparations of 4 Are Described as Those for 4a. *N*-Benzyl-*N*-[2-(*p*-methanesulfonamido phenoxy)ethyl]-*p*-methanesulfonamido Phenethylamine (**4a**). The mixture of methanesulfo chloride (28 mL, 0.361 mol), compound **11a** (35 g, 0.0985 mol), and (Et)₃N (84 mL) in CH₂Cl₂ (280 mL) was stirred overnight, filtered, and condensed. Flash chromatography was performed with acetate–methanol (10:1, v/v), and compound **4a** was given (40 g); yield 78.4%. IR (KBr): 1600, 1500 cm⁻¹. ¹H NMR (DMSO): δ 2.53 (s, 6H), 2.61 (s, 4H), 2.82 (t, 2H), 3.71 (s, 2H), 3.90 (t, 2H), 6.60–6.80 (m, 8H), 7.28 (s, 5H). MS (SCI) data calcd C₂₅H₃₁N₃S₂O₅ m/z (M⁺), 518.1846; found, 518.1818. Anal. (C₂₅H₃₁N₃S₂O₅) C, H, N.

N-Acetyl-*N*-[2-(*p*-methanesulfonamido phenoxy)ethyl]-*p*-methanesulfonamido Phenethylamine (**4b**). IR (KBr): 1640, 1520 cm⁻¹. ¹H NMR (DMSO): δ 1.858, 2.054 (d, 3H), 2.852 (s, 3H), 2.871 (s, 3H), 3.626 (m, 6H), 4.046 (t, 2H), 6.828, 6.931 (d, 2H), 7.122, 7.193 (d, 6H). MS (SCI) data calcd C₂₀H₂₉N₃O₆S₂ m/z (M⁺), 470.4315; found, 470.4362. Anal. (C₂₀H₂₉N₃O₆S₂) C, H, N.

N-[2-(*p*-Methanesulfonamido phenoxy)ethyl]-*p*-methanesulfonamido Phenethylamine (**4c**). The mixture of palladium carbon, compound **4a** (1.5 g, 0.0028 mol), and acetic acid (40 mL) at 30 °C and 15 kg atm was stirred and bubbled by the hydrogen for 8 h, filtered, and neutralized to neutron using alkali and then extracted with acetyl ether; the white compound **4c** (0.5 g) was given; mp 149–151 °C. IR (KBr): 1600, 1510 cm⁻¹. ¹H NMR (CD₃COCD₃): δ 2.811–2.830 (m, 4H), 2.904 (s, 3H), 2.950 (s, 3H), 2.997 (t, 2H), 4.091 (t, 2H), 6.921 (d, 2H), 7.277 (m, 6H). HRMS (SCI) m/z calcd for M⁺, 428.128; found, 428.131. Anal. (C₁₈H₂₅N₃S₂O₅) C, H, N.

N-(*p*-Chlorobenzyl)-*N*-[2-(*p*-methanesulfonamido phenoxy)ethyl]-*p*-methyl-sulfonamido Phenethylamine (**4d**). IR (KBr): 1600, 1520 cm⁻¹. ¹H NMR (DMSO): δ 2.914, 2.9675 (2s, 6H), 3.13, 3.36 (2t, 4H), 3.624 (s, 2H), 4.362 (s, 2H), 4.552 (s, 2H), 7.0 (d, 2H), 7.23 (m, 6H), 7.56–7.70 (dd, 4H). HRMS (SCI) m/z calcd for M⁺, 552.136; found, 552.139. Anal. (C₂₅H₃₀N₃S₂O₅Cl) C, H, N.

N-[2-(*p*-Methanesulfonamido phenoxy)ethyl]-*N*-[2-(*p*-methanesulfonamido phenoxy)ethyl]-*p*-methanesulfonamido Phenethylamine (**4e**). mp 130–133 °C. IR (KBr): 1620, 1520 cm⁻¹. ¹H NMR (DMSO-*d*₆): δ 2.847 (s, 9H), 2.863 (t, 8H), 3.095 (m, 4H), 3.99 (t, 4H), 6.773, 6.882 (d, 4H), 7.141, 7.281 (d, 8H). MS (SCI) m/z 640 (M⁺). Anal. (C₂₇H₃₆O₈S₃N₄) C, H, N.

N-(Methanesulfonamido)-*N*-[2-(*p*-methanesulfonamido phenoxy)ethyl]-*p*-methanesulfonamido Phenethylam-

ine (4f). Compound **4f** was given simultaneously in preparing compound **4e**. IR (KBr): 1600, 1510 cm^{-1} . $^1\text{H NMR}$ ($\text{CDCl}_3 + \text{DMSO}-d_6$): δ 2.858–2.945 (m, 11H), 3.44–3.49 (t, 2H), 3.57–3.66 (t, 2H), 4.03–4.08 (t, 2H), 6.817–6.869 (d, 2H), 7.151–7.219 (m, 6H), 9.318, 9.557 (2s, 2H). MS (SCI) m/z 544 (M^+) (base peak). Anal. ($\text{C}_{19}\text{H}_{27}\text{N}_3\text{S}_2\text{O}_7$) C, H, N.

***N*-Allyl-*N*-[2-(*p*-methanesulfonamido phenoxy)ethyl]-*p*-methanesulfonamido Phenethylamine (4g).** IR (KBr): 1611, 1509 cm^{-1} . $^1\text{H NMR}$ (CDCl_3): δ 2.716 (s, 4H), 2.863 (m, 8H), 3.186 (t, 2H), 3.999–4.06 (t, 2H), 5.05–5.20 (m, 2H), 5.80–5.92 (m, 1H), 6.70–6.784 (m, 2H), 7.062–7.281 (m, 6H). HRMS (SCI) m/z calcd for M^+ , 468.1621; found, 468.1578. Anal. ($\text{C}_{21}\text{H}_{29}\text{N}_3\text{S}_2\text{O}_5$) C, H, N.

***N*-Benzoyl-*N*-[2-(*p*-methanesulfonamido phenoxy)ethyl]-*p*-methanesulfonamido Phenethylamine (4h).** IR (KBr): 1612, 1510 cm^{-1} . $^1\text{H NMR}$ (CDCl_3): δ 2.65–2.85 (m, 7H), 3.5–3.67 (m, 2H), 4.2–4.35 (m, 2H), 6.55–6.6 (m, 2H), 7.18–7.40 (m, 11H). MS (SCI) m/z calcd for M^+ , 454.1795; found, 454.1832. Anal. ($\text{C}_{24}\text{H}_{27}\text{N}_3\text{SO}_4$) C, H, N.

General Procedures for Preparations of 5 Are Described as Those for 5a. ***N*-Methyl-*N*-benzyl-*p*-methanesulfonamido Phenethylamine (5a).** The mixture of methanesulfonamide (0.6 mL, 0.0075 mol), compound **16a** (1.7 g, 0.0071 mol), and $(\text{Et})_3\text{N}$ (2 mL) in CH_2Cl_2 (5 mL) was stirred overnight, filtered, and condensed. Flash chromatography was performed with acetate–methanol (10:1, v/v), and compound **5a** was given (1.75 g); yield 77.6%; mp 97–99 °C. IR (KBr): 1620, 1368 cm^{-1} . $^1\text{H NMR}$ ($\text{CDCl}_3 + \text{DMSO}-d_6$): δ 2.30 (s, 3H), 2.85 (m, 4H), 3.40 (s, 3H), 3.60 (s, 2H), 7.20–7.30 (m, 9H). HRMS (SCI) m/z calcd for M^+ , 319.4420; found, 319.4611. Anal. ($\text{C}_{17}\text{H}_{22}\text{N}_2\text{SO}_2$) C, H, N.

***N*-Methyl-*N*-(*p*-methylbenzyl)-*p*-dimethanesulfonamido Phenethylamine (5b).** In the same manner as described for **5a**, **5b** was prepared from **16b**; mp 102–104 °C. IR (KBr): 1515, 1368 cm^{-1} . $^1\text{H NMR}$ ($\text{CDCl}_3 + \text{DMSO}-d_6$): δ 2.25 (s, 3H), 2.30 (s, 3H), 2.60–2.90 (m, 4H), 3.35 (s, 6H), 3.53 (s, 2H), 7.23–7.44 (m, 8H). HRMS (SCI) m/z calcd for M^+ , 411.2710; found, 411.2691. Anal. ($\text{C}_{19}\text{H}_{26}\text{N}_2\text{S}_2\text{O}_4$) C, H, N.

***N*-Methyl-*N*-(*p*-chlorobenzyl)-*p*-methanesulfonamido Phenethylamine (5c).** In the same manner as described for **5a**, **5c** was prepared from **16c**; mp 59–62 °C. IR (KBr): 1508, 1368 cm^{-1} . $^1\text{H NMR}$ ($\text{CDCl}_3 + \text{DMSO}-d_6$): δ 2.25 (s, 3H), 2.70–2.75 (m, 4H), 3.35 (s, 3H), 3.50 (s, 2H), 7.10–7.40 (m, 8H). HRMS (SCI) m/z calcd for M^+ , 352.8800; found, 352.8820. Anal. ($\text{C}_{17}\text{H}_{21}\text{N}_2\text{SO}_2\text{Cl}$) C, H, N.

***N*-Methyl-*N*-(*p*-methoxybenzyl)-*p*-dimethanesulfonamido Phenethylamine (5d).** IR (KBr): 1616, 1364 cm^{-1} . $^1\text{H NMR}$ ($\text{CDCl}_3 + \text{DMSO}-d_6$): δ 2.25 (s, 3H), 2.83–2.90 (m, 4H), 3.30 (s, 6H), 3.64 (s, 2H), 3.80 (s, 3H), 6.85 (d, 2H), 7.22–7.31 (m, 6H). HRMS (SCI) m/z calcd for M^+ , 427.1400; found, 427.1420. Anal. ($\text{C}_{18}\text{H}_{24}\text{N}_2\text{SO}_3$) C, H, N.

***N*-Methyl-*N*-cyclohexyl-*p*-methanesulfonamido Phenethylamine (5e).** mp 82–86 °C. IR (KBr): 1673, 1372 cm^{-1} . $^1\text{H NMR}$ ($\text{CDCl}_3 + \text{DMSO}-d_6$): δ 1.05–1.90 (m, 11H), 2.35 (s, 3H), 2.80 (m, 4H), 3.05 (s, 3H), 7.30 (m, 4H). HRMS (SCI) m/z calcd for M^+ , 311.4620; found, 311.4590. Anal. ($\text{C}_{16}\text{H}_{25}\text{N}_2\text{SO}_2$) C, H, N.

***N*-Methyl-*N*-(3,4-methylenedioxybenzyl)-*p*-methanesulfonamido Phenethylamine (5f).** mp 115–117 °C. IR (KBr): 1612, 1372 cm^{-1} . $^1\text{H NMR}$ ($\text{CDCl}_3 + \text{DMSO}-d_6$): δ 2.30 (s, 3H), 3.05 (m, 4H), 3.35 (s, 3H), 3.63 (s, 2H), 6.03 (s, 2H), 6.82–7.65 (m, 7H). HRMS (SCI) m/z calcd for M^+ , 363.4410; found, 363.4390. Anal. ($\text{C}_{18}\text{H}_{28}\text{N}_2\text{SO}_4$) C, H, N.

***N*-Benzyl-*N*-(*o*-methoxybenzyl)-*p*-methanesulfonamido Phenethylamine (5g).** mp 96–98 °C. IR (KBr): 2913, 1522 cm^{-1} . $^1\text{H NMR}$ ($\text{CDCl}_3 + \text{DMSO}-d_6$): δ 2.95–3.02 (m, 4H), 3.30 (s, 3H), 3.65 (s, 2H), 3.80 (s, 3H), 3.95 (s, 2H), 7.30–7.85 (m, 13H). HRMS (SCI) m/z calcd for M^+ , 424.3750; found, 424.3790. Anal. ($\text{C}_{24}\text{H}_{28}\text{N}_2\text{SO}_3$) C, H, N.

***N,N*-Dibenzyl-*p*-methanesulfonamido Phenethylamine (5h).** mp 107–111 °C. IR (KBr): 1515, 1368 cm^{-1} . $^1\text{H NMR}$ (CDCl_3): δ 2.85 (m, 4H), 3.35 (s, 3H), 3.65 (s, 4H), 7.25–7.40 (m, 14H). HRMS (SCI) m/z calcd for M^+ , 395.5310; found, 395.5360. Anal. ($\text{C}_{23}\text{H}_{26}\text{N}_2\text{SO}_2$) C, H, N.

***N*-Benzyl-*N*-(*p*-methylbenzyl)-*p*-dimethanesulfonamido Phenethylamine (5i).** mp 112–116 °C. IR (KBr): 1504, 1368 cm^{-1} . $^1\text{H NMR}$ ($\text{CDCl}_3 + \text{DMSO}-d_6$): δ 2.35 (s, 3H), 2.80–2.85 (m, 4H), 3.35 (s, 6H), 4.15 (s, 2H), 4.30 (s, 2H), 7.20–7.55 (m, 13H). HRMS (SCI) m/z calcd for M^+ , 487.2410; found, 487.2470. Anal. ($\text{C}_{24}\text{H}_{28}\text{N}_2\text{SO}_2$) C, H, N.

***N*-Benzyl-*N*-(*p*-chlorobenzyl)-*p*-methanesulfonamido Phenethylamine (5j).** mp 152–154 °C. IR (KBr): 1616, 1364 cm^{-1} . $^1\text{H NMR}$ ($\text{CDCl}_3 + \text{DMSO}-d_6$): δ 2.70 (s, 4H), 3.30 (s, 3H), 3.60 (s, 4H), 7.10–7.40 (m, 13H). HRMS (SCI) m/z calcd for M^+ , 428.9810; found, 428.9890. Anal. ($\text{C}_{23}\text{H}_{25}\text{N}_2\text{SO}_2\text{Cl}$) C, H, N.

***N*-Benzyl-*N*-(*p*-methoxybenzyl)-*p*-dimethanesulfonamido Phenethylamine (5k).** mp 102–106 °C. IR (KBr): 1672, 1284 cm^{-1} . $^1\text{H NMR}$ ($\text{CDCl}_3 + \text{DMSO}-d_6$): δ 2.85 (m, 4H), 3.30 (s, 6H), 3.60 (s, 2H), 3.70 (s, 2H), 3.82 (s, 3H), 6.85 (d, 2H), 7.15–7.30 (m, 11H). HRMS (SCI) m/z calcd for M^+ , 503.5600; found, 503.5620. Anal. ($\text{C}_{25}\text{H}_{30}\text{N}_2\text{S}_2\text{O}_5$) C, H, N.

***N*-Benzyl-*N*-(3,4-methylenedioxybenzyl)-*p*-dimethanesulfonamido Phenethylamine (5l).** mp 122–125 °C. IR (KBr): 1490, 1368 cm^{-1} . $^1\text{H NMR}$ ($\text{CDCl}_3 + \text{DMSO}-d_6$): δ 2.85 (m, 4H), 3.35 (s, 6H), 3.55 (s, 2H), 3.60 (s, 2H), 6.05 (s, 2H), 7.20–7.55 (m, 12H). HRMS (SCI) m/z calcd for M^+ , 517.1500; found, 517.1590. Anal. ($\text{C}_{25}\text{H}_{28}\text{N}_2\text{S}_2\text{O}_6$) C, H, N.

***N*-(*p*-Chlorobenzyl)-*N*-(*p*-methoxybenzyl)-*p*-methanesulfonamido Phenethylamine (5m).** IR (KBr): 1610, 1510 cm^{-1} . $^1\text{H NMR}$ (CDCl_3): δ 2.65 (s, 4H), 2.95 (s, 3H), 3.50 (s, 4H), 3.75 (s, 3H), 6.75–6.85 (d, 2H), 6.95–7.20 (m, 10H). HRMS (SCI) m/z calcd for M^+ , 459.1503; found, 459.1525. Anal. ($\text{C}_{24}\text{H}_{27}\text{N}_2\text{SO}_3\text{Cl}$) C, H, N.

***N*-Methyl-*N*-(*o*-methoxybenzyl)-*p*-methanesulfonamido Phenethylamine (5n).** In the same manner as described for **5a**, **5n** was prepared from **16n**; mp 96–98 °C. IR (KBr): 2913, 1522 cm^{-1} . $^1\text{H NMR}$ ($\text{CDCl}_3 + \text{DMSO}-d_6$): δ 2.30 (s, 3H), 2.95–3.02 (m, 4H), 3.30 (s, 3H), 3.80 (s, 3H), 3.95 (s, 2H), 7.30–7.85 (m, 8H). HRMS (SCI) m/z calcd for M^+ , 349.1583; found, 349.1595. Anal. ($\text{C}_{24}\text{H}_{28}\text{N}_2\text{SO}_3$) C, H, N.

***N*-Acetyl-*N*-(*p*-methoxybenzyl)-*p*-methanesulfonamido Phenethylamine (5o).** Yield 29%; flash chromatography with acetate–petroleum ether (2:1, v/v); $R_f = 0.3$; mp 118–120 °C. IR (KBr): 1618, 1512 cm^{-1} . $^1\text{H NMR}$ (CDCl_3): δ 2.10–2.15 (dd, 3H), 2.85–2.90 (m, 2H), 3.0 (s, 3H), 3.50 (m, 2H), 3.80 (s, 3H), 4.40 (s, 2H), 6.80–7.25 (m, 8H). HRMS (SCI) m/z calcd for M^+ , 376.1451; found, 376.1445. Anal. ($\text{C}_{19}\text{H}_{24}\text{N}_2\text{O}_4\text{S}$) C, H, N.

***N*-Benzoyl-*N*-(*p*-methoxybenzyl)-*p*-methanesulfonamido Phenethylamine (5p).** In the same manner as described for **5a**, **5p** was prepared from **16p**; yield 26%; mp 124–126 °C; flash chromatography with acetate–petroleum ether (1:1, v/v); $R_f = 0.4$. IR (KBr): 1628, 1512 cm^{-1} . $^1\text{H NMR}$ (CDCl_3): δ 2.5–2.9 (m, 5H), 3.50 (s, 2H), 3.70 (s, 3H), 4.30 (s, 2H), 6.60–7.50 (m, 13H). HRMS (SCI) m/z calcd for M^+ , 439.1686; found, 439.1701. Anal. ($\text{C}_{24}\text{H}_{26}\text{N}_2\text{O}_4\text{S}$) C, H, N.

***N*-Methyl-*N*-cyclohexyl-*p*-dimethanesulfonamido Phenethylamine (5q).** Compound **5q** was given simultaneously in preparing compound **5e**. IR (KBr): 1663, 1382 cm^{-1} . $^1\text{H NMR}$ ($\text{CDCl}_3 + \text{DMSO}-d_6$): δ 1.05–1.90 (m, 11H), 2.35 (s, 3H), 2.80 (m, 4H), 3.35 (s, 6H), 7.30 (m, 4H). HRMS (SCI) m/z calcd for M^+ , 389.4620; found, 389.4590. Anal. ($\text{C}_{17}\text{H}_{28}\text{N}_2\text{S}_2\text{O}_4$) C, H, N.

***N,N*-Dibenzyl-*p*-dimethanesulfonamido Phenethylamine (5r).** Compound **5r** was given simultaneously in preparing compound **5h**. IR (KBr): 1615, 1368 cm^{-1} . $^1\text{H NMR}$ (CDCl_3): δ 2.85 (m, 4H), 3.35 (s, 6H), 3.65 (s, 4H), 7.25–7.40 (m, 14H). HRMS (SCI) m/z calcd for M^+ , 473.5310; found, 473.5360. Anal. ($\text{C}_{24}\text{H}_{28}\text{N}_2\text{S}_2\text{O}_4$) C, H, N.

***N*-(*p*-Methoxybenzyl)-*N*-[2-(*p*-methanesulfonamidophenoxy)ethyl]-*p*-methanesulfonamido Phenethylamine (5s).** In the same manner as described for **5a**, **5s** was prepared from **16s**; mp 147–150 °C. IR (KBr): 1600, 1520 cm^{-1} . $^1\text{H NMR}$ (CDCl_3): δ 2.77 (s, 6H), 2.889 (s, 4H), 2.984 (t, 2H), 3.67 (s, 2H), 3.74 (s, 3H), 4.30 (t, 2H), 6.84–6.99 (m, 5H), 7.15–7.22 (m, 7H). HRMS (SCI) m/z calcd for M^+ , 549.2013; found, 549.2061. Anal. ($\text{C}_{24}\text{H}_{29}\text{N}_3\text{O}_2$) C, H, N.

***N*-Methyl-*N*-[2-(naphth-1-yl-oxy)ethyl]-*p*-methanesulfonamido Phenethylamine (6a).** In the same manner as described for **4a**, **6a** was prepared from **20a**; yield 60.3%; flash chromatography CH₃COOC₂H₅/petroleum ether (2:1, v/v); *R*_f = 0.17; mp 130–131 °C. IR (KBr): 1600, 1511 cm⁻¹. ¹H NMR (CDCl₃): δ 2.45 (s, 3H), 2.75–2.85 (2s, 7H), 2.95 (t, 2H), 4.15 (t, 2H), 6.75–6.80 (q, 1H), 7.0–7.4 (m, 6H), 7.55–7.70 (m, 2H), 8.0–8.2 (m, 2H). HRMS (SCI) *m/z* calcd for M⁺, 398.1516; found, 398.1481. Anal. (C₂₂H₂₆N₂SO₃) C, H, N.

***N*-Benzyl-*N*-[2-(naphth-1-yl-oxy)ethyl]-*p*-methanesulfonamido Phenethylamine (6b).** In the same manner as described for **4a**, **6b** was prepared from **21b**; yield 40.7%; flash chromatography CH₃COOC₂H₅/petroleum ether (1:2, v/v); *R*_f = 0.44. IR (KBr): 1579, 1510 cm⁻¹. ¹H NMR (CDCl₃): δ 2.863 (s, 7H), 2.863–3.613 (t, 2H), 3.828 (s, 2H), 4.059–4.163 (t, 2H), 6.740–6.920 (q, 1H), 6.920–7.465 (m, 11H), 7.705 (m, 2H), 8.138–8.179 (m, 2H). HRMS (SCI) *m/z* calcd for M⁺, 475.2059; found, 475.2021. Anal. (C₂₈H₃₀N₂SO₃) C, H, N.

***N*-Acetyl-*N*-[2-(naphth-1-yl-oxy)ethyl]-*p*-methanesulfonamido Phenethylamine (6c).** In the same manner as described for **4a**, **6c** was prepared from **21c**; mp 132–134 °C; yield 81.6%; flash chromatography CH₃COOC₂H₅/petroleum ether (2:1, v/v); *R*_f = 0.28. IR (KBr): 1632, 1509 cm⁻¹. ¹H NMR (CDCl₃): δ 1.95, 2.05 (2s, 3H), 2.90–3.00 (m, 5H), 3.65 (t, 2H), 3.80 (t, 2H), 4.20 (t, 2H), 6.70–6.80 (q, 1H), 7.05–7.45 (m, 11H), 7.60–7.90 (m, 2H), 8.0–8.15 (m, 2H). HRMS (SCI) *m/z* calcd for M⁺, 427.1689; found, 427.1701. Anal. (C₂₃H₂₆N₂SO₄) C, H, N.

***N*-Allyl-*N*-[2-(naphth-1-yl-oxy)ethyl]-*p*-methanesulfonamido Phenethylamine (6d).** In the same manner as described for **4a**, **6d** was prepared from **21d**; yield 20.5%; flash chromatography CH₃COOC₂H₅/petroleum ether (1:2, v/v); *R*_f = 0.22. IR (KBr): 1615, 1504 cm⁻¹. ¹H NMR (CDCl₃): δ 2.85 (s, 4H), 2.90 (s, 3H), 3.05–3.20 (t, 2H), 3.25–3.40 (d, 2H), 4.10–4.20 (m, 2H), 5.10–5.35 (t, 2H), 5.85 (m, 1H), 6.70–6.85 (q, 1H), 7.10–7.50 (m, 8H), 7.70–7.85 (m, 1H), 8.15–8.30 (m, 1H). HRMS (SCI) *m/z* calcd for M⁺, 425.1893; found, 425.1870. Anal. (C₂₄H₂₈N₂SO₃) C, H, N.

***N*-Allyl-*N*-[2-(naphth-1-yl-oxy)ethyl]-*p*-dimethanesulfonamido Phenethylamine (6e).** Compound **6e** was given simultaneously in preparing compound **6d**; yield 20%; flash chromatography CH₃COOC₂H₅/petroleum ether (1:2, v/v); *R*_f = 0.35. IR (KBr): 1579, 1508 cm⁻¹. ¹H NMR (CDCl₃): δ 2.90 (s, 4H), 3.10 (t, 2H), 3.40 (d+s, 8H), 4.15 (t, 2H), 5.10–5.20 (t, 2H), 5.70–5.90 (m, 1H), 6.70–6.85 (q, 1H), 7.15–7.5 (m, 8H), 7.55–7.7 (m, 1H), 8.10–8.30 (m, 1H). HRMS (SCI) *m/z* calcd for M⁺, 503.1663; found, 503.1640. Anal. (C₂₅H₃₀N₂S₂O₅) C, H, N.

***N*-Benzoyl-*N*-[2-(naphth-1-yl-oxy)ethyl]-*p*-methanesulfonamido Phenethylamine (6f).** In the same manner as described for **4a**, **6f** was prepared from **21f**; yield 60.5%; flash chromatography CH₃COOC₂H₅/petroleum ether (1:1, v/v); *R*_f = 0.52. IR (KBr): 1634, 1506 cm⁻¹. ¹H NMR (CDCl₃): δ 2.75 (b, 2H), 3.0 (s, 3H), 3.55 (b, 2H), 3.85 (b, 2H), 4.25 (b, 2H), 6.70 (b, 3H), 7.0–7.40 (m, 9H), 7.50–7.70 (m, 2H), 8.0–8.15 (b, 2H). HRMS (SCI) *m/z* calcd for M⁺, 488.1633; found, 488.1640. Anal. (C₂₈H₂₈N₂SO₄) C, H, N.

***N*-Benzyl-*N*-[2-(naphth-1-yl-oxy)ethyl]-*p*-dimethanesulfonamido Phenethylamine (6g).** Compound **6g** was given simultaneously in preparing compound **6b**. Flash chromatography CH₃COOC₂H₅/petroleum ether (1:2, v/v); *R*_f = 0.6. IR (KBr): 1580, 1508 cm⁻¹. ¹H NMR (CDCl₃): δ 2.85–2.90 (t, 2H), 3.05 (s, 4H), 3.55 (s, 6H), 4.05 (s, 2H), 4.35 (t, 2H), 6.70–6.85 (q, 1H), 7.05–7.50 (m, 11H), 7.60–7.80 (m, 2H), 8.0–8.20 (m, 2H). HRMS (SCI) *m/z* calcd for M⁺, 553.1829; found, 553.1871. Anal. (C₂₉H₃₂N₂S₂O₅) C, H, N.

***N*-Methyl-*N*-[2-(naphth-1-yl-oxy)ethyl]-*p*-dimethanesulfonamido Phenethylamine (6h).** Compound **6h** was given simultaneously in preparing compound **6a**. Flash chromatography CH₃COOC₂H₅/petroleum ether (2:1, v/v); *R*_f = 0.35. IR (KBr): 1582, 1508 cm⁻¹. ¹H NMR (CDCl₃): δ 2.55 (s, 3H), 2.90 (s, 4H), 3.10 (t, 2H), 3.45 (s, 6H), 4.20 (t, 2H), 6.75–6.85 (q, 1H), 7.20–7.50 (m, 6H), 7.70–7.85 (m, 2H), 8.10–8.20

(m, 2H). HRMS (SCI) *m/z* calcd for M⁺, 477.1486; found, 477.1511. Anal. (C₂₃H₂₈N₂S₂O₅) C, H, N.

2-(4-Nitrophenoxy)-1-bromoethane (7). The mixture of 4-nitrophenol (140 g, 1.006 mol), NaOH (40 g), TBA (5 g), and anhydrous alcohol (600 mL) was cooled to 30 °C after it was heated and refluxed for 15 min, added dropwise to 1,2-dibromoethane (250 mL, 2.89 mol), heated, and refluxed for 24 h. Then, the mixture was condensed, filtered, and extracted with acetate. The organic phase was washed with water and dried with anhydrous Na₂SO₄. The condensate was recrystallized in anhydrous alcohol. White crystallized compound (116 g) was given; yield 46.8%; mp 62–64 °C; chromatography CH₃COOC₂H₅/petroleum ether (1:2, v/v); *R*_f = 0.35.

***N*-Acetyl-*p*-nitrophenethylamine.** A mechanically stirred suspension of β-phenethylamine (100 mL, 0.796 mol) was cooled in an ice bath and added dropwise at a rate with acetic anhydride (76 mL, 0.804 mol). It was stirred for 2 h, and the temperature was maintained at 40–45 °C. A stirred mixture of concentrated sulfuric acid (150 mL, 2.81 mol) and concentrated nitric acid (150 mL, 3.33 mol) was added dropwise to the upper solution to the mix acid, continually reacted for 2 h, and then poured into the ice water, extracted three times with acetate, and then combined with the organic phase, dried with anhydrous Na₂SO₄, and condensed. The residue was recrystallized using acetone–water (3:1) to afford the desired product; white acicular crystal 76 g; yield 46.0%; mp 138–140 °C; Merk Index *p*-NO₂C₆H₄CH₂CH₂NHAc mp 138 °C.

***p*-Nitrophenethylamine Hydrobromide (8).** A 47% (v/v) amount of hydrobromic acid (110 mL, 0.75 mol) was added to *N*-acetyl-*p*-nitrophenethylamine (60 g, 0.288 mol), and the solution was refluxed for 6 h by stirring and heating and then cooled at room temperature, and a white powder appeared; weight 71 g; yield 99%; mp 218 °C; Merk Index *p*-NO₂C₆H₄CH₂CH₂NH₂ mp 27 °C.

***N*-[2-(*p*-Nitrophenoxy)ethyl]-*p*-nitrophenethylamine (9).** The mixture of compound **8** (40.0 g, 0.162 mol), compound **7** (32 g, 0.13 mol), and K₂CO₃ (33 g, 0.239 mol) in acetonitrile (160 mL) was stirred at room temperature overnight. The reaction mixture was poured into ice water and adjusted to pH 2 with 10% HCl. The precipitated solid was recrystallized with acetic ether/petroleum ether, and then, a yellowish powder was given (43.5 g); yield 81.5%; chromatography CH₃COOC₂H₅/petroleum ether (2:1, v/v); *R*_f = 0.4; mp 58–60 °C.

General Procedures for Preparations of 10 Are Described as Those for 10a. ***N*-Benzyl-*N*-[2-(*p*-nitrophenoxy)ethyl]-*p*-nitrophenethylamine (10a).** The mixture of compound **9** (10 g, 0.0302 mol) and K₂CO₃ (6 g, 0.044 mol) in CH₃CN (100 mL) was added to C₆H₅CH₂Cl (3.54 g, 0.028 mol) and stirred and refluxed for 3.5 h. The reaction mixture was filtered and condensed. Flash chromatography with acetate–petroleum ether was performed (4:1, v/v); *R*_f = 0.7. Compound **10a** was given (3.6 g); yield 61%; mp 94–96 °C. IR (KBr): 1600, 1510 cm⁻¹. ¹H NMR (CDCl₃): δ 2.912 (s, 4H), 2.98 (t, 2H), 3.76 (s, 2H), 4.03 (t, 2H), 6.885 (m, 2H), 7.261–7.30 (m, 7H), 8.1–8.2 (m, 4H). MS (SCI) *m/z* 422 (M⁺).

***N*-Acetyl-*N*-[2-(*p*-nitrophenoxy)ethyl]-*p*-nitrophenethylamine (10b).** Yield 91%; flash chromatography with acetate–petroleum ether (1:1, v/v); *R*_f = 0.45; mp 112–113 °C. IR (KBr): 1600, 1520 cm⁻¹. ¹H NMR (CDCl₃): δ 2.04, 2.21 (d, 3H), 3.04 (t, 2H), 3.72 (m, 4H), 4.03–4.30 (m, 2H), 6.88–6.98 (m, 2H), 7.20–7.48 (m, 2H), 8.01–8.29 (m, 4H). MS (SCI) *m/z* 374 (M⁺).

***N*-(*p*-Chlorobenzyl)-*N*-[2-(*p*-nitrophenoxy)ethyl]-*p*-nitrophenethylamine (10d).** Yield 50%; flash chromatography with acetate–petroleum ether (1:2, v/v); *R*_f = 0.70; mp 96–98 °C. IR (KBr): 1600, 1510 cm⁻¹. ¹H NMR (DMSO): δ 2.87 (s, 4H), 2.95 (t, 2H), 3.23 (s, 2H), 4.00 (t, 2H), 6.89 (d, 2H), 7.2–7.4 (m, 6H), 8.0–8.4 (m, 4H). MS (SCI) *m/z* 458 (M²⁺).

***N*-[2-(*p*-Nitrophenoxy)ethyl]-*N*-[2-(*p*-nitrophenoxy)ethyl]-*p*-nitrophenethylamine (10e).** Flash chromatography with acetate–petroleum ether (1:1, v/v); *R*_f = 0.45, was performed, and the yellow solid was given; mp 110–113 °C. IR (KBr): 1600, 1510 cm⁻¹. ¹H NMR (CDCl₃): δ 2.98 (s, 8H),

3.08 (t, 4H), 4.06 (t, 4H), 6.80–6.87 (d, 2H), 7.30–7.37 (d, 2H), 8.00–8.17 (m, 6H). MS (SCI) m/z 497 (M^+).

***N*-Allyl-*N*-[2-(*p*-nitrophenoxy)ethyl]-*p*-nitrophenethylamine (10g).** Flash chromatography with acetate–petroleum ether (1:1, v/v), $R_f = 0.35$, was performed, and the yellow solid was given. IR (KBr): 1605, 1510 cm^{-1} . $^1\text{H NMR}$ (CDCl_3): δ 2.80 (s, 4H), 2.86 (m, 2H), 3.13 (t, 2H), 4.06 (t, 2H), 5.10 (m, 2H), 5.90 (m, 1H), 6.80–6.87 (d, 2H), 7.30–7.37 (m, 6H). MS (SCI) m/z 371 (M^+).

***N*-Benzoyl-*N*-[2-(*p*-nitrophenoxy)ethyl]-*p*-nitrophenethylamine (10h).** mp 82–84 °C. $^1\text{H NMR}$ (CDCl_3): δ 3.024 (m, 2H), 3.779, 3.849 (m, 4H), 4.220 (m, 2H), 7.086–7.454 (m, 9H), 8.075–8.247 (m, 4H).

General Procedures for Preparations of 11 Are Described as Those for 11a. ***N*-Benzyl-*N*-[2-(*p*-aminophenoxy)ethyl]-*p*-(amino)phenethylamine (11a).** The mixture of acetone (50 mL), hydrochloric acid (1 mL), reductive iron powder (5 g, 0.089 mol), and a little ammonium chloride was stirred and boiled for 0.5 h and cooled to 45 °C, and then, a solution of compound 10a (8.14 g, 0.0217 mol) in 50 mL of acetone was added to the mixture dropwise over 3 h. The reaction mixture was cooled and adjusted to pH 10 with 10% NaOH, then filtered, and condensed. Flash chromatography with acetate–petroleum ether (1:1, v/v) was performed, and compound 11a was given (5.1 g); yield 87%. $^1\text{H NMR}$ (CDCl_3): δ 2.8 (s, 4H), 3.0 (t, 2H), 3.73 (s, 2H), 3.87 (t, 2H), 6.9–7.0 (m, 8H), 7.27 (s, 5H). MS (SCI) m/z 362 (M^+) (base peak).

***N*-Acetyl-*N*-[2-(*p*-aminophenoxy)ethyl]-*p*-(amino)phenethylamine (11b).** Yield 78%; flash chromatography with acetate–petroleum ether (1:1, v/v); $R_f = 0.33$. $^1\text{H NMR}$ (CDCl_3): δ 1.92, 2.15, (d, 3H), 2.75 (t, 2H), 3.41–3.62 (q, 4H), 4.03 (t, 2H), 6.57–6.68 (m, 6H), 6.89–7.01 (m, 2H). MS (SCI) m/z 314 (M^+).

General Procedures for Preparations of 14 Are Described as Those for 14a. ***N*-Benzyl-*p*-nitrophenethylamine Hydrochloride (14a).** The mixture of *p*-nitrophenylethylamine (10 g, 0.06 mol), benzaldehyde (5.8 mL, 0.06 mol), and anhydrous ethanol (50 mL) was heated and stirred for 2 h and then cooled, and KBH_4 (3 g) was added and reacted for 5 h. The reaction was cooled and filtered, and the yellow solid was given (15.1 g); yield 86%; mp 256–258 °C. $^1\text{H NMR}$ ($\text{CDCl}_3 + \text{DMSO-}d_6$): δ 3.20 (s, 4H), 4.15 (dd, 2H), 7.20–7.85 (m, 7H), 8.15 (d, 2H).

***N*-(*p*-Methylbenzyl)-*p*-nitrophenethylamine Hydrochloride (14b).** In the same manner as described for 14a, 14b was prepared from *p*-methyl-benzaldehyde; mp 246–248 °C. $^1\text{H NMR}$ ($\text{CDCl}_3 + \text{DMSO-}d_6$): δ 2.35 (s, 3H), 3.00–3.40 (m, 4H), 3.83 (s, 2H), 7.10 (d, 2H), 7.30 (d, 2H), 7.49 (d, 2H), 8.12 (d, 2H).

***N*-(*p*-Chlorobenzyl)-*p*-nitrophenethylamine Hydrochloride (14c).** In the same manner as described for 14a, 14c was prepared from *p*-chloro-benzaldehyde; mp 203–205 °C. $^1\text{H NMR}$ ($\text{CDCl}_3 + \text{DMSO-}d_6$): δ 3.22 (m, 4H), 4.40 (s, 2H), 7.44–8.25 (m, 8H).

***N*-(*p*-Methoxybenzyl)-*p*-nitrophenethylamine Hydrochloride (14d).** In the same manner as described for 14a, 14d was prepared from *p*-methoxy-benzaldehyde; mp 246–248 °C. $^1\text{H NMR}$ ($\text{CDCl}_3 + \text{DMSO-}d_6$): δ 3.45 (m, 4H), 3.85 (s, 3H), 4.10 (s, 2H), 6.90 (d, 2H), 7.20–7.40 (m, 4H), 8.15 (d, 2H).

***N*-(Cyclohexyl)-*p*-nitrophenethylamine Hydrochloride (14e).** In the same manner as described for 14a, 14e was prepared from cyclohexanone; mp 180–182 °C. $^1\text{H NMR}$ ($\text{CDCl}_3 + \text{DMSO-}d_6$): δ 1.05–2.34 (m, 11H), 3.34–3.40 (m, 4H), 7.50 (d, 2H), 8.12 (d, 2H), 9.50 (bro, 1H, D_2O exchangeable).

***N*-(3,4-Methylenedioxybenzyl)-*p*-nitrophenethylamine Hydrochloride (14f).** In the same manner as described for 14a, 14f was prepared from 3,4-methylenedioxy benzaldehyde; mp 242–246 °C. $^1\text{H NMR}$ ($\text{CDCl}_3 + \text{DMSO-}d_6$): δ 3.20–3.40 (m, 4H), 4.05 (s, 2H), 6.10 (s, 2H), 6.80 (d, 2H), 7.10 (d, 2H), 7.28 (s, 1H), 7.52 (d, 2H), 8.15 (d, 2H).

***N*-(*o*-Methoxybenzyl)-*p*-nitrophenethylamine Hydrochloride (14g).** In the same manner as described for 14a, 14g was prepared from *o*-methoxy benzaldehyde; mp 179–182 °C.

$^1\text{H NMR}$ ($\text{CDCl}_3 + \text{DMSO-}d_6$): δ 3.20–3.25 (m, 4H), 3.65 (s, 3H), 3.90 (s, 2H), 7.15–8.15 (m, 8H).

***N*-(*p*-Methoxybenzyl)-*p*-nitrophenethylamine Hydrochloride (14o).** The mixture of *p*-nitrophenylethylamine (30 g, 0.18 mol), benzene (90 mL, 24.19 mL, 0.19 mol), and anisaldehyde was stirred and refluxed for 4 h and then cooled, and ethanol (120 mL) and KBH_4 (9 g) were added, and it was refluxed for 2 h. The reaction was cooled and then adjusted to pH 3 and filtered, and the white solid was given (50 g); yield 85.8%; mp 230–232 °C. IR (KBr): 1600, 1510 cm^{-1} . $^1\text{H NMR}$ (CDCl_3): δ 2.91 (s, 4H), 3.74 (s, 2H), 3.78 (s, 3H), 6.78–6.9 (m, 2H), 7.1–7.4 (m, 4H), 8.0–8.2 (m, 2H).

General Procedures for Preparations of 15a–g Are Described as Those for 15a. ***N*-Methyl-*N*-benzyl-*p*-nitrophenethylamine Hydrochloride (15a).** A 36% formaldehyde (11 mL, 0.16 mol) amount was added to compound 14a (10 g, 0.034 mol) in formic acid 88% (6.4 mL, 0.21 mol), it was heated and refluxed for 4 h, and then, it was adjusted to a solution of pH 14 with 20% NaOH, extracted with acetate, and condensed. Flash chromatography with acetate–petroleum ether (2:1, v/v) was performed, and compound 15a was given (9.5 g); yield 92.3%; mp 218–220 °C. $^1\text{H NMR}$ ($\text{CDCl}_3 + \text{DMSO-}d_6$): δ 2.75 (s, 3H), 3.15 (s, 4H), 4.20 (s, 2H), 7.45–7.78 (m, 7H), 8.15 (d, 2H).

***N*-Methyl-*N*-(*p*-methylbenzyl)-*p*-nitrophenethylamine Hydrochloride (15b).** In the same manner as described for 15a, 15b was prepared from 14b; mp 185–186.5 °C. $^1\text{H NMR}$ ($\text{CDCl}_3 + \text{DMSO-}d_6$): δ 2.30 (s, 3H), 2.65 (s, 3H), 3.35 (s, 4H), 4.40 (q, 2H), 7.20–7.60 (m, 6H), 8.12 (d, 2H).

***N*-Methyl-*N*-(*p*-chlorobenzyl)-*p*-nitrophenethylamine Hydrochloride (15c).** In the same manner as described for 15a, 15c was prepared from 14c; mp 146–150 °C. $^1\text{H NMR}$ ($\text{CDCl}_3 + \text{DMSO-}d_6$): δ 2.80 (s, 3H), 3.35 (s, 2H), 3.40 (s, 2H), 4.40 (s, 2H), 7.30–7.85 (m, 6H), 8.12 (d, 2H).

***N*-Methyl-*N*-(*p*-methoxybenzyl)-*p*-nitrophenethylamine Hydrochloride (15d).** mp 170–172 °C. $^1\text{H NMR}$ ($\text{CDCl}_3 + \text{DMSO-}d_6$): δ 2.70 (s, 3H), 3.25 (s, 4H), 3.75 (s, 3H), 4.30 (q, 2H), 6.95 (d, 2H), 7.54 (d, 4H), 8.15 (d, 2H).

***N*-Methyl-*N*-cyclohexyl-*p*-nitrophenethylamine Hydrochloride (15e).** mp 214–217 °C. $^1\text{H NMR}$ ($\text{CDCl}_3 + \text{DMSO-}d_6$): δ 1.15–2.30 (m, 11H), 2.70 (s, 3H), 3.20–3.35 (m, 4H), 7.60 (d, 2H), 8.15 (d, 2H).

***N*-Methyl-*N*-(3,4-methylenedioxybenzyl)-*p*-nitrophenethylamine Hydrochloride (15f).** mp 208–209 °C. $^1\text{H NMR}$ ($\text{CDCl}_3 + \text{DMSO-}d_6$): δ 2.70 (s, 3H), 3.25 (s, 2H), 3.30 (s, 2H), 4.28 (q, 2H), 6.05 (s, 2H), 6.81 (d, 1H), 7.08 (d, 1H), 7.25 (s, 1H), 7.51 (d, 2H), 8.15 (d, 2H).

***N*-Benzyl-*N*-(*o*-methoxybenzyl)-*p*-nitrophenethylamine Hydrochloride (15g).** mp 168–169 °C. $^1\text{H NMR}$ ($\text{CDCl}_3 + \text{DMSO-}d_6$): δ 3.20 (s, 4H), 3.65 (s, 2H), 3.83 (s, 3H), 4.05 (q, 2H), 7.30–8.15 (m, 13H).

General Procedures for Preparations of (15h–m,o,p) Are Described as Those for 15h. ***N,N*-Dibenzyl-*p*-nitrophenethylamine Hydrochloride (15h).** To the mixture of compound 14a (10 g, 0.034 mol) and K_2CO_3 (8.3 g, 0.06 mol) in anhydrous ethanol (50 mL) was added $\text{C}_6\text{H}_5\text{CH}_2\text{Br}$ (4.5 mL, 0.03 mol), and it was stirred and refluxed for 3.5 h. The reaction mixture was filtered and condensed. Flash chromatography with acetate–petroleum ether (4:1, v/v), $R_f = 0.45$, was performed, and compound 15h was given (11.8 g); yield 91.3%; mp 186–189 °C. $^1\text{H NMR}$ ($\text{CDCl}_3 + \text{DMSO-}d_6$): δ 3.30 (s, 2H), 3.36 (s, 2H), 4.45 (s, 4H), 7.2–8.15 (m, 14H).

***N*-Benzyl-*N*-(*p*-methylbenzyl)-*p*-nitrophenethylamine Hydrochloride (15i).** In the same manner as described for 15h, 15i was prepared from 14b; mp 212–214 °C. $^1\text{H NMR}$ ($\text{CDCl}_3 + \text{DMSO-}d_6$): δ 2.25 (s, 3H), 3.30–3.35 (m, 4H), 4.30–4.55 (d, 4H), 7.25–8.10 (m, 13H).

***N*-Benzyl-*N*-(*p*-chlorobenzyl)-*p*-nitrophenethylamine Hydrochloride (15j).** In the same manner as described for 15h, 15j was prepared from 14c; mp 168–172 °C. $^1\text{H NMR}$ ($\text{CDCl}_3 + \text{DMSO-}d_6$): δ 3.40 (m, 4H), 4.50 (s, 4H), 7.45–8.10 (m, 13H).

***N*-Benzyl-*N*-(*p*-methoxybenzyl)-*p*-nitrophenethylamine Hydrochloride (15k).** In the same manner as de-

scribed for **15h**, **15k** was prepared from **14d**; mp 166–169 °C. ¹H NMR (CD₃COCD₃): δ 3.32–3.48 (m, 4H), 3.80 (s, 3H), 4.40–4.50 (d, 4H), 7.00 (d, 2H), 7.55–7.98 (m, 9H), 8.12 (d, 2H).

N-Benzyl-N-(3,4-methylenedioxybenzyl)-p-nitrophenethylamine Hydrochloride (15l). In the same manner as described for **15h**, **15l** was prepared from **14f**; mp 166–169 °C. ¹H NMR (CDCl₃): δ 3.20–3.25 (m, 4H), 4.20 (s, 4H), 6.05 (s, 2H), 7.0–8.0 (m, 12H).

N-(p-Chlorobenzyl)-N-(p-methoxybenzyl)-p-nitrophenethylamine Hydrochloride (15m). In the same manner as described for **15h**, **15l** was prepared from **14d**; mp 166–169 °C. ¹H NMR (CDCl₃): δ 2.65 (s, 4H), 3.55 (s, 4H), 3.80 (s, 3H), 6.5–6.6 (dd, 2H), 6.75–6.9 (m, 4H), 7.10–7.30 (m, 6H).

N-Methyl-N-(o-methoxybenzyl)-p-nitrophenethylamine Hydrochloride (15n). In the same manner as described for **15a**, **15n** was prepared from **14g**; mp 168–169 °C. ¹H NMR (CDCl₃ + DMSO-*d*₆): δ 2.70 (s, 3H), 3.20 (s, 4H), 3.83 (s, 3H), 4.05 (s, 2H), 7.30–8.15 (m, 8H).

N-Acetyl-N-(p-methoxybenzyl)-p-nitrophenethylamine (15o). In the same manner as described for **15h**, **15o** was prepared from **14o** (1.6 g) and acetic oxide. We were given a yellow solid (1.6 g); yield 97%; flash chromatography with acetate–petroleum ether (1:1, v/v); *R*_f = 0.3; mp 68–70 °C. ¹H NMR (CDCl₃): δ 2.05, 2.10 (d, 3H), 2.95–3.0 (m, 2H), 3.50 (m, 2H), 3.80 (s, 3H), 4.40 (s, 2H), 6.80–7.30 (m, 6H), 8.10–8.15 (m, 2H).

N-Benzoyl-N-(p-methoxybenzyl)-p-nitrophenethylamine (15p). In the same manner as described for **15h**, **15p** was prepared from **14o** (3 g) and benzoyl chloride, and a yellow solid was given (1.1 g); yield 26%; flash chromatography with acetate–petroleum ether (1:2, v/v); *R*_f = 0.3; mp 100–102 °C. ¹H NMR (CDCl₃): δ 2.90–3.0 (s, 2H), 3.50 (s, 2H), 3.80 (s, 3H), 4.45 (s, 2H), 6.80–6.90 (d, 2H), 7.2–7.4 (m, 9H), 8.0–8.2 (d, 2H).

N-(p-Methoxybenzyl)-N-[2-(p-nitrophenoxy)ethyl]-p-nitrophenethylamine Hydrochloride (15s). In the same manner as described for **10a**, **15s** was prepared from **14o**; yield 45.7%; mp 91–93 °C. IR (KBr): 1600, 1520 cm⁻¹. ¹H NMR (CDCl₃): δ 2.90 (s, 4H), 3.00 (t, 2H), 3.73 (s, 2H), 3.76 (s, 3H), 4.167 (t, 2H), 6.819–7.52 (m, 6H), 8.06–8.20 (m, 6H).

General Procedures for Preparations of 16 Are Described as Those for 16a. N-Methyl-N-benzyl-p-(amino)phenethylamine Hydrochloride (16a). The mixture of acetone (50 mL), hydrochloric acid (1 mL), reductive iron powder (6 g, 0.107 mol), and a little ammonium chloride was stirred and boiled for 0.5 h and cooled to 45 °C, and then, a solution of compound **15a** (4.0 g) in 50 mL of acetone was added to the mixture dropwise over 3 h. The reaction mixture was cooled and adjusted to pH 10 with 10% NaOH and then filtered and condensed. Flash chromatography with acetate–petroleum ether (1:1, v/v) was performed, and compound **16a** was given (3.4 g); yield 93.7%; mp 264–265 °C. ¹H NMR (DMSO-*d*₆): δ 2.65 (s, 3H), 3.15 (s, 4H), 4.38 (s, 2H), 7.20–7.72 (m, 9H).

N-Methyl-N-(p-methylbenzyl)-p-(amino)phenethylamine Hydrochloride (16b). In the same manner as described for **16a**, **16b** was prepared from **15b**; mp 267–270 °C. ¹H NMR (DMSO-*d*₆): δ 2.30 (s, 3H), 2.65 (s, 3H), 3.10 (s, 4H), 4.33 (q, 2H), 7.20–7.58 (m, 8H).

N-Methyl-N-(p-chlorobenzyl)-p-(amino)phenethylamine Hydrochloride (16c). In the same manner as described for **16a**, **16c** was prepared from **15c**; mp 261–263 °C. ¹H NMR (DMSO-*d*₆): δ 2.70 (s, 3H), 3.20–3.25 (m, 4H), 4.30 (s, 2H), 6.92 (d, 2H), 7.11 (d, 2H), 7.42 (d, 2H), 7.69 (d, 2H).

N-Methyl-N-(p-methoxybenzyl)-p-(amino)phenethylamine Hydrochloride (16d). mp 257–258 °C. ¹H NMR (CDCl₃ + DMSO-*d*₆): δ 2.70 (s, 3H), 3.20–3.25 (m, 4H), 3.83 (s, 3H), 4.30 (q, 2H), 6.91 (d, 2H), 7.20–7.40 (m, 4H), 7.52 (d, 2H).

N-Methyl-N-cyclohexyl-p-(amino)phenethylamine Hydrochloride (16e). mp 264–266 °C. ¹H NMR (CDCl₃ + DMSO-*d*₆): δ 1.05–2.40 (m, 11H), 2.80 (s, 3H), 3.00–3.30 (m, 4H), 7.38 (q, 4H).

N-Methyl-N-(3,4-methylenedioxybenzyl)-p-(amino)phenethylamine Hydrochloride (16f). mp 258–260 °C. ¹H NMR (DMSO-*d*₆): δ 2.65 (s, 3H), 3.20 (s, 4H), 4.15 (q, 2H), 6.10 (s, 2H), 6.90–7.40 (m, 7H).

N-Benzyl-N-(o-methoxybenzyl)-p-(amino)phenethylamine Hydrochloride (16g). mp 245–247 °C. ¹H NMR (DMSO-*d*₆): δ 3.05–3.10 (m, 4H), 3.65 (s, 2H), 3.75 (s, 3H), 4.02 (s, 2H), 7.27–7.90 (m, 13H).

N,N-Dibenzyl-p-(amino)phenethylamine Hydrochloride (16h). mp 222–224 °C. ¹H NMR (CDCl₃): δ 3.14 (s, 4H), 4.40 (s, 4H), 7.08 (d, 2H), 7.22–7.80 (m, 12H).

N-Benzyl-N-(p-methylbenzyl)-p-(amino)phenethylamine Hydrochloride (16i). mp 252–256 °C. ¹H NMR (CDCl₃ + DMSO-*d*₆): δ 2.30 (s, 3H), 3.00 (s, 4H), 4.12 (s, 2H), 4.15 (s, 2H), 6.65–7.55 (m, 13H).

N-Benzyl-N-(p-chlorobenzyl)-p-(amino)phenethylamine Hydrochloride (16j). mp 207–209 °C. ¹H NMR (CDCl₃): δ 3.25 (s, 4H), 4.35 (s, 2H), 4.43 (s, 2H), 7.20–7.85 (m, 13H).

N-Benzyl-N-(p-methoxybenzyl)-p-(amino)phenethylamine Hydrochloride (16k). mp 234–236 °C. ¹H NMR (CDCl₃ + DMSO-*d*₆): δ 2.95 (s, 4H), 3.70 (s, 3H), 3.90 (s, 2H), 3.95 (s, 2H), 7.55–7.88 (m, 13H).

N-Benzyl-N-(3,4-methylenedioxybenzyl)-p-(amino)phenethylamine Hydrochloride (16l). mp 217–219 °C. ¹H NMR (CDCl₃): δ 3.10–3.15 (m, 4H), 4.35 (s, 4H), 6.05 (s, 2H), 7.0–7.75 (m, 12H).

N-(p-Chlorobenzyl)-N-(p-methoxybenzyl)-p-(amino)phenethylamine (16m). In the same manner as described for **16a**, **16m** was prepared from **15m**. ¹H NMR (CDCl₃): δ 2.65 (s, 4H), 3.55 (s, 4H), 3.80 (s, 3H), 6.5–6.6 (dd, 2H), 6.75–6.9 (m, 4H), 7.10–7.30 (m, 6H).

N-Methyl-N-(o-methoxybenzyl)-p-(amino)phenethylamine Hydrochloride (16n). mp 245–247 °C. ¹H NMR (DMSO-*d*₆): δ 2.55 (s, 3H), 3.05–3.10 (m, 4H), 3.75 (s, 3H), 4.02 (s, 2H), 7.27–7.90 (m, 8H).

N-Acetyl-N-(p-methoxybenzyl)-p-(amino)phenethylamine (16o). Yield 80%; flash chromatography with acetate–petroleum ether (2:1, v/v); *R*_f = 0.5.

N-(p-Methoxybenzyl)-N-[2-(p-aminophenoxy)ethyl]-p-(amino)phenethylamine (16s). In the same manner as described for **16a**, **16s** was prepared from **15s**. MS (SCI) *m/z* 392 (M⁺).

1-Bromo-2-(naphth-1-yl-oxy)ethane (18). The mixture of 4-nitrophenol α-naphthol (**17**) (20 g, 0.1387 mol), NaOH (5.7 g), TBA (5 g), and anhydrous alcohol (85 mL) was cooled to 30 °C after it was heated and refluxed for 15 min; 1,2-dibromoethane (34.5 mL, 0.398 mol) was added dropwise, heated, and refluxed for 24 h, and it was condensed, filtered, and extracted. The organic phase was washed with water and dried (anhydrous Na₂SO₄) and recrystallized in anhydrous alcohol. White crystallized compound (16.5 g) was given; yield 47.4%; mp 62–64 °C. Flash chromatography CH₃COOC₂H₅/petroleum ether (1:4, v/v); *R*_f = 0.8. MS (SCI) *m/z* 252 (MH⁺), 115 (base peak).

N-[2-(Naphth-1-yl-oxy)ethyl]-p-nitrophenethylamine (19). In the same manner as described for **9**, **19** was prepared from **18**. Flash chromatography CH₃COOC₂H₅/petroleum ether (1:4, v/v); *R*_f = 0.48.

N-Methyl-N-[2-(naphth-1-yl-oxy)ethyl]-p-nitrophenethylamine (20a). A 36% amount of formaldehyde (3.7 mL, 0.0448 mol) was added to compound **19** (4.42 g, 0.0132 mol) in formic acid 88% (2.6 mL, 0.0606 mol), and it was heated and refluxed for 4 h, then adjusted solution to pH 14 with 20% NaOH, extracted with acetate, and condensed. Flash chromatography with acetate–petroleum ether (2:1, v/v) was performed, and compound **20a** was given (2.2 g); yield 47.6%; flash chromatography CH₃COOC₂H₅/petroleum ether (1:1, v/v); *R*_f = 0.45. ¹H NMR (CDCl₃): δ 2.5 (s, 3H), 2.95 (s, 4H), 3.0 (t, 2H), 4.20 (t, 2H), 6.70–6.80 (q, 1H), 7.20–7.45 (m, 6H), 7.70–7.80 (m, 2H), 7.95–8.20 (m, 2H).

N-Benzyl-N-[2-(naphth-1-yl-oxy)ethyl]-p-nitrophenethylamine (20b). In the same manner as described for **10a**, **20b** was prepared from **19**; yield 65.9%; mp 58–60 °C; flash chromatography CH₃COOC₂H₅/petroleum ether (2:1, v/v); *R*_f

= 0.65. $^1\text{H NMR}$ (CD_3COCD_3): δ 2.95 (s, 4H), 3.05 (t, 2H), 3.75 (s, 2H), 4.15 (t, 2H), 6.65–6.80 (q, 1H), 7.10–7.50 (m, 11H), 7.70–8.0 (m, 3H), 8.10–8.25 (m, 1H).

N-Acetyl-N-[2-(naphth-1-yl-oxy)ethyl]-p-nitrophenethylamine (20c). In the same manner as described for **10b**, **20c** was prepared from **19**; mp 60–62 °C; flash chromatography $\text{CH}_3\text{COOC}_2\text{H}_5$ /petroleum ether (1:5, v/v); R_f = 0.73. $^1\text{H NMR}$ (CD_3COCD_3): δ 1.95, 2.20 (2s, 3H), 3.10 (m, 2H), 3.70–3.90 (m, 4H), 4.15–4.40 (m, 2H), 6.80–6.90 (m, 1H), 7.25–7.50 (m, 6H), 7.65–7.85 (m, 1H), 7.95–8.25 (m, 3H).

N-Allyl-N-[2-(naphth-1-yl-oxy)ethyl]-p-nitrophenethylamine (20d). In the same manner as described for **10b**, **20d** was prepared from **19**; mp 60–62 °C; flash chromatography $\text{CH}_3\text{COOC}_2\text{H}_5$ /petroleum ether (1:5, v/v); R_f = 0.45. $^1\text{H NMR}$ (CD_3COCD_3): δ 2.95 (m, 4H), 3.05–3.15 (t, 2H), 3.25–3.40 (t, 2H), 4.15–4.20 (t, 2H), 5.10–5.35 (t, 2H), 5.85 (m, 1H), 6.70–6.85 (q, 1H), 7.10–7.50 (m, 8H), 7.70–7.85 (m, 1H), 8.15–8.30 (m, 1H).

N-Benzoyl-N-[2-(naphth-1-yl-oxy)ethyl]-p-nitrophenethylamine (20f). In the same manner as described for **10a**, **20f** was prepared from **19**; yellow oil; yield 66.2%; flash chromatography $\text{CH}_3\text{COOC}_2\text{H}_5$ /petroleum ether (1:2, v/v); R_f = 0.27. $^1\text{H NMR}$ (CD_3COCD_3): δ 3.10 (s, 2H), 3.90 (b, 4H), 4.40 (b, 2H), 6.90 (b, 1H), 7.20–7.60 (m, 11H), 7.75–7.90 (m, 2H), 8.0–8.20 (m, 2H).

N-Benzyl-N-[2-(naphth-1-yl-oxy)ethyl]-p-(amino)phenethylamine (21b). In the same manner as described for **11a**, **21b** was prepared from **20b**; yield 59%; flash chromatography $\text{CH}_3\text{COOC}_2\text{H}_5$ /petroleum ether (1:4, v/v); R_f = 0.36.

N-Benzoyl-N-[2-(naphth-1-yl-oxy)ethyl]-p-(amino)phenethylamine (21f). In the same manner as described for **11a**, **21f** was prepared from **20f**; yield 50%; flash chromatography $\text{CH}_3\text{COOC}_2\text{H}_5$ /petroleum ether (1:2, v/v); R_f = 0.38. MS (SCI) data calcd $\text{C}_{27}\text{H}_{26}\text{N}_2\text{O}_2$ m/z (M^+), 411.2063; found, 411.2040.

Acknowledgment. We gratefully acknowledge financial support from the National Natural Science Foundation of China (Grants 29725203 and 20072042), the State Key Program of Basic Research of China (Grant 1998051115), the Life Science Foundation for Young Scientists of CAS (Grant STZ-00-06), the Qi Ming Xiang Foundation of Shanghai Ministry of Science and Technology (Grant 00QB14034), and the Postdoctoral Fellowship of Shanghai. The calculations were performed on a Power challenge server at the Network Information Center, Chinese Academy of Science, Shanghai Branch. We also thank Madam Frances Sue Payton for improving the English.

References

- Newman, W. P.; Tracy, R. E.; Strong, J. P.; Johnson, W. D.; Oalman, M. C. Pathology of sudden coronary death. *Ann. N. Y. Acad. Sci.* **1982**, *382*, 39–49.
- Kaplan, H. R. Advances in antiarrhythmic drug therapy-changing concepts. *Fed. Proc.* **1986**, *45*, 2184–2185.
- Panidis, I. P.; Morganroth, J. Sudden death in hospitalized patients: cardiac rhythm disturbances detected by ambulatory electrocardiographic monitoring. *J. Am. Coll. Cardiol.* **1983**, *2*, 798–805.
- Pratt, C. M.; Francis, M. J.; Luck, J. C.; Wyndham, C. R.; Miller, R. R.; Quinones, M. A. Analysis of ambulatory electrocardiograms in 15 patients during spontaneous ventricular fibrillation with special reference to preceding arrhythmic events. *J. Am. Coll. Cardiol.* **1983**, *2*, 789–797.
- Carmeliet, E.; Mubagwa, K. Antiarrhythmic drugs and cardiac ion channels: mechanisms of action. *Prog. Biophys. Mol. Biol.* **1998**, *70*, 1–72.
- Vaughan Williams, E. M. A Classification of antiarrhythmic drugs reassessed after a decade of new Drugs. *J. Clin. Pharmacol.* **1984**, *24*, 129–147.
- Rasmusson, R. L.; Morales, M. J.; Wang, S.; Liu, S.; Campbell, D. L.; Brahmajothi, M. V.; Strauss, H. C. Inactivation of voltage-gated cardiac K^+ channels. *Circ. Res.* **1998**, *82*, 739–750.
- Echt, D. S.; Liebson, P. R.; Mitchell, L. B.; Peters, R. W.; Obias Manno, D.; Barker, A. H.; Arensberg, D.; Baker, A.; Friedman, L.; Greene, H. L. Mortality and Morbidity in Patients Receiving Encainide, Flecainide, or Placebo-The Cardiac Arrhythmia Suppression Trial. *N. Engl. J. Med.* **1991**, *324*, 781–788.
- Woolley, R. L. CAST: Implications for drug development. *Clin. Pharmacol. Ther.* **1990**, *47*, 553–556.
- Vaughan Williams, E. M. Delayed ventricular repolarization as an antiarrhythmic principle. *Eur. Heart J.* **1985**, *6* (Suppl. D), 145–149.
- Thomas, J. C. Antiarrhythmic drugs: where are we going? Technical Review. *Pharm. News* **1995**, *2*, 17–23.
- Sanguinetti, M. C.; Jurkiewicz, N. K. Two components of cardiac delayed rectifier K^+ current. *J. Gen. Physiol.* **1990**, *96*, 195–215.
- Sanguinetti, M. C.; Curran, M. E.; Zou, A.; Shen, J.; Spector, P. S.; Atkinson, D. L.; Keating, M. T. Coassembly of $\text{K}(\text{V})\text{LQT1}$ and minK (IsK) proteins to form cardiac I(Ks) potassium channel. *Nature* **1996**, *384*, 80–83.
- Moses, C. Advanced partial life support controversy: where do antiarrhythmic agents fit in? *Pharmacotherapy* **1997**, *20*, 84–87.
- Hindricks, G.; Kottkamp, H.; Haverkamp, W.; Shenasa, M.; Shenasa, H.; Borggrefe, M.; Breithardt, G. Magnesium-electrophysiological effects, antiarrhythmic properties and clinical applications. In *Antiarrhythmic Drugs*, 2nd ed.; Breithardt, G., Borggrefe, M., Camm, A. J., Shenasa, M., Eds.; Springer-Verlag Berlin Heidelberg: Germany, 1995; pp 363–392.
- Lazzara, R. From first class to third class: recent upheaval in antiarrhythmic therapy—lessons from clinical trials. *Am. J. Cardiol.* **1996**, *78*, 28–33.
- Phillips, G. B.; Morgan, T. K.; Nickisch, K.; Lind, J. M.; Gomez, R. P.; Wohl, R. A.; Argentieri, T. M.; Sullivan, M. E. Synthesis and cardiac electrophysiological activity of aryl-substituted derivatives of the class III antiarrhythmic agent sematilide. Potential class I/III agents. *J. Med. Chem.* **1990**, *33*, 627–633.
- Selnick, H. G.; Liverton, N. J.; Baldwin, J. J.; Butcher, J. W.; Claremon, D. A.; Elliott, J. M.; Freidinger, R. M.; King, S. A.; Libby, B. E.; McIntyre, C. J.; Pribush, D. A.; Remy, D. C.; Smith, G. R.; Tebben, A. J.; Jurkiewicz, N. K.; Lynch, J. J.; Salata, J. J.; Sanguinetti, M. C.; Siegl, P. K.; Slaughter, D. E.; Vyas, K. Class III antiarrhythmic activity in vivo by selective blockade of the slowly activating cardiac delayed rectifier potassium current IKs by (*R*)-2-(2,4-trifluoromethyl)-*N*-[2-oxo-5-phenyl-1-(2,2,2-trifluoroethyl)-2,3-dihydro-1H-benzo[*e*][1,4]diazepin-3-yl]-acetamide. *J. Med. Chem.* **1997**, *40*, 3865–3868.
- Saher, D. I.; Reiffel, J. A.; Bigger, J. T.; Squatrito, A.; Kidwell, G. A. Efficacy, safety, and tolerance of *d*-Sotalol in patients with refractory supraventricular tachyarrhythmias. *Am. Heart J.* **1989**, *117*, 562–568.
- Cross, P. E.; Arrowsmith, J. E.; Thomas, G. N.; Gwilt, M.; Burges, R. A.; Higgins, A. J. Selective class III antiarrhythmic agents. 1 Bis(arylalkyl)amines. *J. Med. Chem.* **1990**, *33*, 1151–1155.
- Gwilt, M.; Blackburn, K. J.; Burges, R. A.; Higgins, A. J.; Milne, A. A. Electropharmacology of dofetilide, a new class III agent, in anaesthetized dogs. *Eur. J. Pharmacol.* **1992**, *215*, 137–144.
- Knilans, T. K.; Lathrop, D. A.; Nanasi, P. P.; Schwartz, A.; Varro, A. Rate and concentration-dependent effects of UK-68,798, a potent new class III antiarrhythmic, on canine purkinje fibre action potential duration and V_{max} . *Br. J. Pharmacol.* **1991**, *103*, 1568–1572.
- Baskin, E. P.; Lynch, J. J. Comparative effects of increased extracellular potassium and pacing frequency on the class III activities of methanesulfonanilide IKr blockers dofetilide, D-sotalol, E-4031, and MK-499. *J. Cardiovasc. Pharmacol.* **1994**, *24*, 199–208.
- Wallace, A. A.; Stupienski, R. F.; Brookes, L. M.; Selnick, H. G.; Claremon, D. A.; Lynch, J. J. Cardiac electrophysiologic and inotropic actions of new and potent methanesulfonanilide class III antiarrhythmic agents in anesthetized dogs. *J. Cardiovasc. Pharmacol.* **1991**, *18*, 687–695.
- Smith, D. A.; Rasmussen, H. S.; Stopher, D. A.; Walker, D. K. Pharmacokinetics and metabolism of dofetilide in mouse, rat, dog and man. *Xenobiotica* **1992**, *22*, 709–719.
- Gwilt, M.; Arrowsmith, J. E.; Blackburn, K. J.; Burges, R. A.; Cross, P. E.; Dalrymple, H. W.; Higgins, A. J. UK-68, 798: a novel, potent and highly selective class III antiarrhythmic agent which blocks potassium channels in cardiac Cells. *J. Pharmacol. Exp. Ther.* **1991**, *256*, 318–324.

- (27) Abrahamsson, C.; Palmer, M.; Ljung, B.; Duker, G.; Baarnhielm, C.; Carlsson, L.; Danielsson, B. Induction of rhythm abnormalities in the fetal rat heart. A tentative mechanism for the embryotoxic effect of the class III antiarrhythmic agent almokalant. *Cardiovasc. Res.* **1994**, *28*, 337–344.
- (28) Jurkiewicz, N. K.; Sanguinetti, M. C. Rate dependent prolongation of cardiac action potentials by a methanesulfonanilide class III antiarrhythmic agent. Specific block of a rapidly activating delayed rectifier K^+ current by dofetilide. *Circ. Res.* **1993**, *72*, 75–83.
- (29) Liu, H.; Ji, M.; Jiang, H. L.; Liu, L. G.; Hua, W. Y.; Chen, K. X.; Ji, R. Y. Computer-aided design, synthesis and biological assay of *p*-methylsulfonamido phenylethylamine analogues. *Bioorg. Med. Chem. Lett.* **2000**, *10*, 2153–2157.
- (30) Cramer, D. R., III; Paterson, D. E.; Bunce, J. D. Comparative molecular field analysis (CoMFA). I. Effect of shape on binding of steroids to carried proteins. *J. Am. Chem. Soc.* **1988**, *110*, 5959–5967.
- (31) Klebe, G.; Abraham, U.; Mietzner, T. Molecular similarity indices in a comparative analysis (CoMSIA) of drug molecules to correlate and predict their biological activity. *J. Med. Chem.* **1994**, *37*, 4130–4146.
- (32) Tong, W.; Lewis, D. R.; Perkins, R.; Chen, Y.; Welsh, W. J.; Goddette, D. W.; Heritage, T. W.; Sheehan, D. M. Evaluation of quantitative structure–activity relationship methods for large-scale prediction of chemicals binding to the estrogen receptor. *J. Chem. Inf. Comput. Sci.* **1998**, *38*, 669–677.
- (33) Wettwer, E.; Scholtysik, G.; Schaad, A.; Himmel, H.; Ravens, U. Effects of the new class III antiarrhythmic drug E-4031 on myocardial contractility and electrophysiological parameters. *J. Cardiovasc. Pharmacol.* **1991**, *17*, 480–487.
- (34) Johnson, R. E.; Silver, P. J.; Becker, R.; Birsner, N. C.; Bohnet, E. A.; Briggs, G. M.; Busacca, C. A.; Canniff, P.; Carabateas, P. M.; Chadwick, C. C.; Ambra, T. D.; Dundore, R. L.; Dung, J. S.; Ezrin, A. M.; Gorczyca, W.; Habeeb, P. G.; Krafte, P. H. D. S.; Pilling, G. M.; Connor, B. O.; Saindane, M. T.; Schlegel, D. C.; Stankus, G. P.; Swestock, J.; Volberg, W. A. 4,5-Dihydro-3-(methanesulfonamidophenyl)-1-phenyl-1H-2,4-benzodiazepines: a novel class III antiarrhythmic agents. *J. Med. Chem.* **1995**, *38*, 2551–2556.
- (35) *Sybyl*, version 6.7; Tripos Associates: St. Louis, MO, 2000.
- (36) Purcel, W. P.; Singer, J. A. *J. Chem. Eng. Data* **1967**, *12*, 235–246. Details of the implementation are given in *Sybyl 6.5 Theory Manual*; Tripos Associates: St. Louis, MO, 1998; p 69.
- (37) Stahle, L. Wold, S. Multivariate analysis and experimental design in biochemical research. *Prog. Med. Chem.* **1988**, *25*, 292–337.
- (38) Cramer, R. D., III. Partial least squares (PLS) strengths and limitations. *Perspect. Drug Discovery Des.* **1993**, *1*, 269–278.
- (39) Kiyama, R.; Tamura, Y.; Watanabe, F.; Tsuzuki, H.; Ohtani, M.; Yodo, M. Homology modeling of gelatinase catalytic domains and docking simulations of novel sulfonamide inhibitors. *J. Med. Chem.* **1999**, *42*, 1723–1738.
- (40) Matter, H.; Schwab, W.; Barbier, D.; Billen, G.; Haase, B.; Neises, B.; Schudok, M.; Thorwart, W.; Schreuder, H.; Brachvogel, V.; Lonze, P.; Weithmann, K. U. Quantitative structure–activity relationship of human neutrophil collagenase (MMP-8) inhibitors using comparative molecular field analysis and X-ray structure analysis. *J. Med. Chem.* **1999**, *42*, 1908–1920.
- (41) Jiang, H. L.; Chen, K. X.; Tang, Y.; Chen, J. Z.; Li, Q.; Wang, Q. M.; Ji, R. Y. Molecular modeling and 3D-QSAR studies on the interaction mechanism of tripeptidyl thrombin inhibitors with human α -thrombin. *J. Med. Chem.* **1997**, *40*, 3085–3090.
- (42) POV-ray Team; *POV-ray*, version 3; 1999 (www.povray.org).
- (43) Kobertz, W. R.; Miller, C. K^+ channels lacking the 'tetramerization' domain: implications for pore structure. *Nat. Struct. Biol.* **1999**, *6*, 1122–1125.

JM010574U